

for vitrification and disposal. The original salt solution that was fed to the process, now free of the actinides, can be recycled.

Biocatalytic Destruction of Nitrate. The presence of high nitrate (NO_3^-) and nitrite (NO_2^-) concentrations, often of the order of 4 M, in DOE mixed waste streams creates problems in establishing suitable final waste forms and disposal modes. Disposal of low-level wastes by near-surface grouting requires grout formulations that will minimize the leachability of the nitrates, and the vitrification process for high-level wastes to form ceramic glasses produces volatile nitrogen oxides in the off-gases. The objective of this work was to convert the nitrates and nitrites to oxygen and water by use of nitrate, nitrite, and nitrous oxide reductase enzymes. Such enzymes result in very high specific catalytic activity without a need for additional chemical reagents or production of secondary waste streams.

In this process, an aqueous biphasic system consisting of a salt-rich aqueous phase and a PEG-rich aqueous phase is used to protect the enzymes and to facilitate removal of the nitrate/nitrite from the waste stream. The enzymes stay in the PEG phase, where they are not exposed to the high ionic strength of the waste stream. The nitrates and nitrites transfer into the PEG phase while the radionuclides remain in the salt phase. A schematic illustration of the process is shown in Fig. 6-7.

The enzymes are immobilized on the surface of an electrode, and an electron-transfer agent, which is also immobilized on the electrode surface, shuttles electrons from the electrode to the enzyme. The overall chemical reaction for the reduction of nitrate to nitrogen is

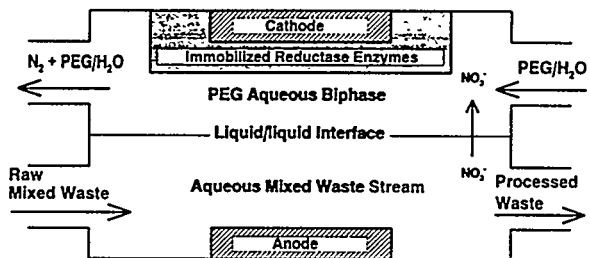
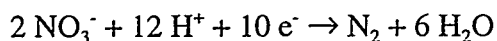


Fig. 6-7. Schematic for Biocatalytic Destruction of Nitrate

The reaction occurs through a sequence of steps, $\text{NO}_3^- \rightarrow \text{NO}_2^- \rightarrow \text{N}_2\text{O} \rightarrow \text{N}_2$, so any nitrite or N_2O in the waste stream will also be reduced. The reductase and electron-transfer agent were immobilized on the gold electrode surface by an electrodeposition procedure. The enzymes retained their catalytic activity over an extended period. Plans were made to demonstrate the process on a surrogate waste stream. The aqueous biphasic studies were led by Dave Chaiko. Others involved in the work were Adam Ellison, Gary Henriksen, John Kopasz, Ted Krause, Robert Mensah-Biney, Carol Mertz, and Erv Van Deventer.

ELECTROKINETIC PROCESSES

A major problem at DOE sites is the presence of metals, particularly actinides and transuranics, and/or hazardous organic compounds such as chlorinated and aromatic hydrocarbons in the soil. Electrokinetics, which refers to the movement of charged particles through a porous medium under the influence of an applied electric field, offers the possibility of *in situ* remediation of contaminated soils. The two principal forms of electrokinetics are electroosmosis and electrophoresis. The DOE had asked ANL to investigate a soil decontamination process being developed by Isotron Coating Technology of New Orleans, Louisiana. This procedure, called the "Electro-sorb Soil Decontamination Process," involved the superimposition of oscillating waves, either

electromagnetic (*e.g.*, microwave or electric power) or mechanical (*e.g.*, sonic or ultrasonic), on a normal dc electric field. Argonne was to determine whether the superimposed waves did, in fact, enhance the electrokinetic recovery process.

Argonne proposed a separate study to develop electrokinetic processes to enhance the molecular transport rates in systems of this type. The ANL effort was to investigate novel catalysts to destroy or detoxify hazardous organic chemicals in contaminated soils and groundwaters. A major engineering challenge was to bring the catalyst and the contaminant in contact in the soils, which are complex structures that inhibit transport rates and complicate flow patterns. These effects can be minimized by applying an electrical potential to the system to generate an electroosmotic flow.

The overall efficiency of the electrokinetic process depended on a multiplicity of variables, including the mobilities of ions and charged particles, viscosity of the groundwater, ion concentration, hydration of ions and charged particles, dielectric constant of the medium, and the temperature.

Experiments were initiated on the effect of temperature on the efficiency of electrokinetic remediation for the extraction of potassium dichromate ($K_2Cr_2O_7$) from kaolinite samples. This system was selected in anticipation of a future field demonstration on a chromate waste site at Sandia National Laboratories. In general, the rate of chromium migration was increased by raising the temperature (from 21 to 55°C). The overall results were complicated, however, by the many physical and chemical mechanisms involved in the system.

Some work was done on the use of silica gel barriers to inhibit the migration of contaminants, such as radionuclides, heavy metals, and hazardous organic compounds, through soil subsurface as a means of environmental remediation and waste

management. The silica gel barriers are formed by destabilizing a colloidal silica sol by two steps—lowering the pH and increasing the salt concentration. Hydraulic pumping is used to inject the sol mixture into the soil, but it presents a number of difficulties, including the need for multiple cycles to fill all the pores and problems in controlling the flow of the sol solution. Electrokinetic methods of injecting the sol appeared to be an attractive alternative to pumping because the electroosmotic effect fills all the pores uniformly, and the transport can be controlled by the positions of the electrodes in the soil. In bench-scale electrokinetic tests at Lehigh University, the procedure resulted in a great decrease in the permeability of the soil, but in kaolinite soil the permeability actually increased. The kaolinite fibers were not cemented, and silica gel fibers were extruded from the sample.

CHEMICALLY BONDED WASTE FORMS

A cooperative project between the Energy Technology (ET) Division and CMT was undertaken to evaluate the suitability of phosphate inorganic binders for solidification and stabilization of mixed wastes (heavy metals and actinides) that are not suitable for thermal processes. The rationale was that certain phosphate mineral phases such as monazites and apatite occur in natural environments and can incorporate thorium, uranium, and rare earth elements. Samples of magnesium and zirconium phosphate waste forms containing Cd, Cr, Ni, and Pb were subjected to standard leaching tests. Untreated ash greatly exceeded the EPA limits, while the treated material was well below the limits.

The fact that these phosphate wastes contain water of crystallization led to concerns that hydrogen might be produced. In addition to hydrogen production, oxygen depletion occurred in the vessels, which were

filled with air. Much of the oxygen was in the form of CO and CO₂, and more was consumed by formation of water and other condensable molecules.

An alternative approach to converting the zeolite wastes into an acceptable waste form for storage was to incorporate the zeolite into a low-temperature phosphate glass. Zinc phosphate, which has a glass-transition temperature in the range of 325-375°C, was a candidate glass for this purpose. Small-scale composite monoliths containing cesium-loaded crystalline silicotitanate, zeolite, and sodalite were prepared by cold pressing and sintering at 460°C. Cesium release from these materials in standard 3-day leach tests was extremely low. Other test indicated that cesium has about the same fractional release rate as Zn, Na, K, and Li from the salt-free glass. These studies were led by Don Reed. Others involved in the effort were Allen Bakel, Edgar Buck, Jim Cunnane, Don Fischer, Terry Johnson, and Michele Lewis.

RADIOLYTIC GAS-GENERATION STUDIES

Radiolytic gas-generation studies are being conducted on a chemically bonded phosphate ceramic called "Ceramicrete," which is being developed for encapsulation of TRU-bearing wastes. Radiation from the radionuclides produces hydrogen and smaller amounts of other gases by radiolysis of water and other materials present in the waste form. Among the experiments that were performed was a comparison of the hydrogen produced in a plutonium-loaded Ceramicrete sample. The sample, which originally contained 18.9 wt% H₂O, had a G value of 0.37 molecules H₂/100 eV, but when the sample was dried to a water content of about 1 wt%, the G value was only 0.04 molecules of H₂/100 eV. Other types of samples gave somewhat mixed results, and further work is in progress.

ACTINIDE STABILITY/SOLUBILITY STUDIES

The Waste Isolation Pilot Plant (WIPP), located in Carlsbad, New Mexico, is a possible disposal site for TRU radioactive wastes. Studies were undertaken to provide experimental data for WIPP on actinide solubilities and oxidation-state distributions in WIPP brines having pH values between 5 and 10. Steady-state concentrations of Pu(VI) were maintained in the brine over the 18-month duration of the experiments. Additions of reducing agents relevant to the WIPP reduced the Pu(VI) to Pu(IV) and lowered the steady-state concentrations of plutonium in the brine solutions.

Organic chelating agents expected to be present in the brines also caused the reduction of Pu(VI) and Pu(IV). Work is continuing in collaboration with Sandia National Laboratories in which the long-term data that are generated are being used to challenge their high-ionic-strength models for actinide solubility.

ACTINIDE SPECIATION IN GROUNDWATER

These studies, which involved at various stages the collaboration of Pacific Northwest Laboratory, Brookhaven National Laboratory, Lawrence Berkeley Laboratory, and Northwestern University, were concerned with the speciation (*i.e.*, complexation, oxidation states, and aggregation) of radionuclides under conditions relevant to the subsurface groundwaters at DOE installations. The initial investigations were aimed at the hydrolysis of Pu(VI), which was known to be much more soluble than Pu(IV) and was therefore more likely to have high migration rates in the soil. Those studies were followed by investigations of the interactions of Pu(VI) with organic complexing agents that were likely to be present in the soil as a

consequence of plutonium processing operations. That work led into studies of the effects of microbes on the plutonium reactions and the effects of plutonium on the microbes. These studies employed high-intensity laser spectroscopic methods supplemented by several more conventional spectroscopic and radiochemical methods.

Because of some uncertainty as to whether the hydrolysis product of Pu(VI) was PuO_2OH^+ or $(\text{PuO}_2\text{OH})_2^{2+}$, spectroscopic measurements were made on the hydrolysis products of Pu(VI) in 0.1 M sodium perchlorate solution as a function of pH, Pu(VI) concentration, and temperature. Increasing the pH above 3 resulted in the formation of hydrolysis products; four distinct species were found in the pH range of 3 to 7. The extent of hydrolysis and the contribution of polynuclear hydrolysis products were much larger than previously thought. The temperature variable measurements (10-45°C) led to the first experimental determinations of the thermochemical properties of the hydrolysis products. The effect of temperature was much less than previous estimates in the literature.

The interactions of Pu(VI) with organic complexing agents (citric acid and acetohydroxamic acid) in aqueous systems were examined as a function of pH. At pH greater than 2, the Pu(VI) was reduced to Pu(III) by the acetohydroxamic acid and to Pu(IV) by the citric acid. In further work on the citrate system, the interaction of Pu(VI) with citric acid was investigated as a function of ligand-to-metal ratio (1:1 to 100:1) and pH (2 to 10). At ligand-to-metal ratios of less than 10:1, citrate reduced the Pu(VI) to form a stable Pu(IV) complex, and the reaction rate became higher with increasing pH. At ligand-to-metal ratios of about 100:1, no Pu(VI) reduction occurred, even at near-neutral pH, which suggests that multiligand complexation of the Pu(VI) stabilizes the oxidation state.

Some preliminary studies were conducted on the degradation of the plutonium citrate

and nitrilotriacetic acid (NTA) complexes by a *Pseudomonas* strain microbe. A stable Pu(IV)-citrate complex that was not biotically oxidized or reduced was observed, and about 20% of the plutonium initially present was associated with the microbe. In the case of the NTA complex, the existence of the complex did not prevent conversion of the NTA to CO_2 , but it decreased the reaction rate slightly. The NTA complex was of particular interest because NTA was a complexing agent associated with plutonium processing. At near-neutral pH (6 to 8), the Pu(IV)-NTA complex was stable over a period of months. In the presence of the *chelatorbacter* microbe, however, the NTA was metabolized, destabilizing the complex and forming plutonium polymers. A set of conditions was established in such a way that the rate of the biodegradation process could be monitored by monitoring the CO_2 formation. Up to 80% of the plutonium was associated with the microbial fraction after the reaction.

The radiation tolerance of the microbes was a factor of importance to this work. In the NTA growth medium, the presence of plutonium proved to have a detrimental effect, with a survivability of less than 1% at the highest plutonium concentrations ($10^{-5}M$). The radiation tolerance of the *halobium* microbe, which was being considered for use in the bioremediation of DOE sites, was evaluated by measuring the survivability as a function of absorbed doses of gamma radiation. The radiation tolerance of this microbe was about 1 Mrad, which led to the conclusion that only radiation from the uptake of plutonium caused radiation damage when plutonium was the sole source of ionizing radiation. This study was followed by an investigation of the interactions of the plutonium-NTA complex with the *Chelatobacter heintzii*, which was known to be a degrader of the NTA complexant. Increasing concentrations of plutonium up to 0.01 mM resulted in a lower rate of NTA

degradation. The NTA tied up in the plutonium complex was not readily accessible to the microbe for degradation, and the ionizing radiation reduced the survivability of the microbes.

In a continuation of this work, gamma irradiation experiments showed that over 99% of the *C. heintzii* bacteria was killed by an exposure of 18.5×10^3 rad. When Pu-242 was substituted for Pu-239, the cell death rate was proportional to the activity of the plutonium rather than to its concentration. The plutonium radiation dose to kill the bacteria was far less than the gamma dose. Apparently, association of plutonium with the bacteria was a critical step in the loss of cell viability in that alpha-particle deposition in or near the cell was needed to account for the toxicity. At low plutonium concentrations ($<10^{-4}$ mM), bioassociation of the plutonium was rapid and occurred even in the presence of the NTA complexing agent. At higher plutonium concentrations, association of the plutonium with the biomass was slow and was attributed to destabilization of the Pu-NTA complex and subsequent plutonium polymer formation. An effort was undertaken at Northwestern University to develop a biodegradation model that would assist in correlating data and developing a more comprehensive picture of the biodegradation processes.

In 1997, work continued on the interactions of multivalent actinide species with bacteria. Investigations were conducted on the interaction of the actinide-nitrilotriacetic (NTA) complex with the NTA-degrading microbe *Chelatobacter heintzii* in aqueous solution. This research involved extensive integration of computer modeling with laboratory experiments. Results to date show that actinide toxicity depends upon the oxidation state and isotope of the actinide. For example, Pu(IV) toxicity is radiolytic in nature, while Np(V) toxicity is chemical and similar to that of other heavy metals.

The actinide speciation work, under Don Reed, included Del Bowers, Jim Cunnane, Jim Helt, Shigeo Okajima, and Mike Richmann.

OFFICE OF WASTE MANAGEMENT

The Office of Waste Management in CMT assisted DOE in a national applied R&D program of environmental restoration and waste management. The objective was to improve the efficiency, safety, and timeliness of environmental cleanup activities so as to meet DOE's 30-year environmental compliance and cleanup goals. This activity consisted of technical and management support to the Minimum Additive Waste Stabilization (MAWS) Program and the Hazardous Substance Research Center (HSRC) Program, which was co-funded by DOE and the Environmental Protection Agency (EPA). The objective of the MAWS program was to separate the hazardous from the nonhazardous components of the waste and vitrify the hazardous portion in a small volume. The MAWS technology had potential application to a wide variety of DOE wastes such as soils, tank wastes, sludge pits, ashes, and asbestos at various sites, including Hanford, Savannah River, Rocky Flats, Oak Ridge, and Fernald. The HSRC program involved five HSRCs in different regions of the country, each one being located at the site of a main university in a consortium of universities. The research in this program was wide-ranging, but all aimed at developing a better understanding of the nature of the contaminated areas and different approaches to remedial actions. A third task was then added to this program in the form of technical assistance to DOE and coordination of information from the Integrated Program for Development of In-Situ Remediation Technologies. This office was disbanded in 1995. Jim Helt bore the primary responsibility for this effort.

PERSONNEL

Other participants in the above programs include the following: Scott Aase, Jim Banaszak, John Basco, John Bates, Nick Beskid, Dave Chamberlain, Cliff Conner, Jim Cunnane, Jas Devgun, Bill Ebert, Jeff Emery, Bob Finch, Pat Finn, Jeff Fortner, Margaret Goldberg, Lohman Hafenrichter, Mark Hash, Joe Hoh, Lester Morss, Michael Nole, Kevin Quigley, John Quinn, Lin Simpson, Shiu-Wing Tam, and Stephen Wolf. Kevin Byrne, Martin Clemens, Sheldon Lee, Jian Shu Luo, and Paul Nelson worked on the design of an unvented reactor for the incineration or vitrification of hazardous and mixed radioactive wastes. In addition to these people, a large number of part-time and temporary personnel were involved in this effort.

Nuclear Waste Management

In the 1990s, CMT investigators continued their studies of the corrosion behavior of nuclear waste slated for disposal in the proposed Yucca Mountain Repository in southwestern Nevada. In these studies, a variety of tests were performed on the corrosion of simulated high-level waste glasses and spent nuclear fuel under an unsaturated water environment typical of that in the proposed repository. Tests were also conducted to support development of vitrified forms for the disposal of low-level waste generated at the DOE Hanford site, as well as glasses for disposal of surplus plutonium and plutonium-bearing wastes. Contaminated soils at various sites, such as the Fernald plant in Ohio, were characterized to aid in the remediation of those sites.

John Bates was in charge of this work in the early 1990s, reporting first to Jim Battles, then to Jim Laidler, followed by Terry Johnson, and much of the success of the program can be attributed to John's influence.

In 1994, Denis Strachan was appointed as Acting Manager of the Waste Management Department, which included Hazardous Waste Management under Jim Cunnane, Nuclear Waste Management under Denis Strachan, and Separation Science and Technology under George Vandegrift. In 1998, Robert Einziger became the head of this department.

TESTING OF HIGH-LEVEL WASTE GLASSES

In long-term test programs, some of which were begun in the 1980s, the corrosion behavior of high-level waste glasses upon exposure to water or water vapor has been followed continuously. As of 1996, some glasses had been under test for 12 years. The purpose of this work was to assist DOE in the qualification of high-level waste glasses for disposal in the Yucca Mountain Repository. The work was aimed primarily at glass compositions similar to those produced at the Savannah River Site in the Defense Waste Processing Facility (DWPF) and at the West Valley Demonstration Project. Other glasses under test are an Environmental Assessment glass, a benchmark glass produced in the DWPF, and a radioactive glass incorporating a Hanford tank sludge. The information obtained from these tests is to be used to predict the long-term (>10,000-y) behavior of high-level glasses under conditions typical of what may be expected in the Yucca Mountain Repository.

Static Dissolution Tests of High-Level Waste Glasses. Borosilicate glass has been chosen as the vitrification material for confining transuranic elements and fission products. Static dissolution tests with simulated high-level wastes are in progress at 90°C and at several sample surface area/solution volume (S/V) ratios. The corrosion mechanism is inferred from the release rate of the glass matrix

elements (Li, Na, B, and Si) and the radionuclides, solution pH, and alteration phases that form on the glass surface. (Alteration phases are a variety of minerals, such as hydrates, silicates, and zeolites that form on the glass surface as a result of reaction of the base material with water and dissolved constituents in the water.) In tests up to five years at S/V ratios of 340 and 2,000 m⁻¹, alteration layers formed on both radioactive and nonradioactive Savannah River glasses (SRL 131), but two other glasses of different composition (SRL 165 and 200) had not reached the alteration formation stage. At a S/V ratio of 20,000 m⁻¹, alteration phases had formed on the nonradioactive SRL 200 glass, but not on its radioactive homologue, a difference attributed to a lower pH (by 0.5 to 1.0 pH unit) in the leachate for the radioactive glass. This lower pH is believed to have resulted from radiolysis in the air and solution. An important finding in these tests is that the dissolution rate of the glass increases markedly after alteration phases have formed on the glass.

The disposition of radionuclides is determined primarily by their solution chemistries. Both plutonium and americium are sparingly soluble in the alkaline solutions generated during these tests, while uranium and neptunium are moderately soluble. Significant amounts of these actinides become associated with colloidal material resulting from spallation of the alteration phases, and settle out over time. The solubility of technetium is high in short-term tests, but decreases as test times are extended to longer than one year.

In tests of an Environmental Assessment glass, alteration phases formed within one year at a S/V ratio of 2000 m⁻¹ and within 14 days at a S/V ratio of 20,000 m⁻¹. Unlike the SRL glasses, the dissolution rate decreased with time after formation of the alteration phases for unknown reasons.

The results of various tests were interpreted in terms of a reaction progress variable that reflects the transformation of glass to more thermodynamically stable alteration phases. In the first stage of corrosion, the glass dissolves at a rate controlled by its composition, the solution pH, and temperature. In the second stage, the rate is controlled by the buildup of dissolved glass components. The formation of alteration phases may affect the dissolution rate in the third stage. Several glasses have shown corrosion increasing to a high rate after zeolites and other phases form. Preliminary results from a model that has been developed to relate glass composition to its long-term corrosion behavior are promising.

Drip Tests of Savannah River and West Valley Glasses. Drip tests of an actinide- and technetium-doped Savannah River glass (SRL 165) were begun and were still in progress in 1998. Designed to simulate potential conditions in the proposed Yucca Mountain Repository, groundwater representative of the site (EJ-13 well water equilibrated with volcanic tuff) is slowly dripped onto glass samples at 90°C in a closed stainless steel vessel. Release of the glass components, including the actinides, is monitored by periodic analyses of the leachate. The procedure and equipment were described in Chapter 5. Insoluble elements, including U, Pu, and Am, are incorporated into alteration phases as the glass reacts and are subsequently released with particulate or colloidal matter as the alteration phases spall from the glass. Recent trends have shown that the release rates of Pu and Am, while initially low, accelerate as the alteration phases spall from the surface. As shown in Fig. 6-8, the increase in their release rates began at about the eighth year of testing. Ultimately, the transport of these actinides from the waste form will depend on the transport of particles and colloids suspended in solutions.

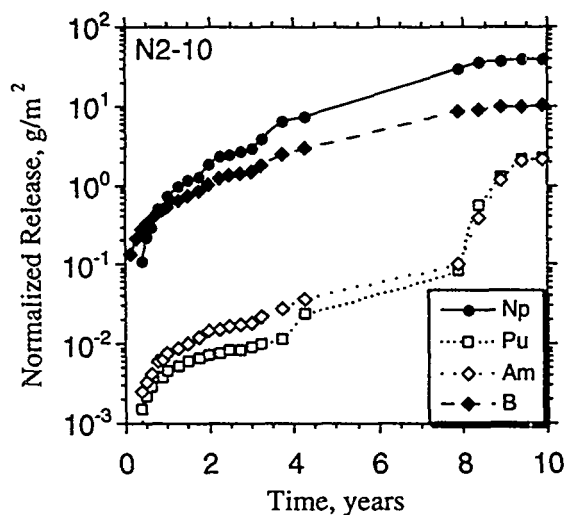


Fig. 6-8. Release of Boron and Actinide Elements from Waste Glass by Leaching

Similar drip tests were conducted with a West Valley glass (ATM 10), beginning in 1987. This glass contains a substantial amount of thorium, which was incorporated into the alteration phases as CaThPO_4 and as thorium-titanium-iron silicates. These alteration phases appear to play a substantial role in corrosion of the glass as the element thorium was released to the test solution at a rate nearly three orders of magnitude lower than the water-soluble elements, lithium and boron.

As of 1998, after more than ten years of drip testing, the data indicate that the insoluble elements (U, Pu, and Am) were incorporated into alteration phases as the glass reacted and were subsequently released with particulate or colloidal matter as the alteration products spalled from the glass. The more recent trends showed that releases of Pu and Am, although quite low initially compared to those of the soluble elements such as B and Np, become accelerated as the alteration phases spall off the glass surfaces and enter the test solution. Release of technetium, which is a fission product of concern because of its migration characteristics, was similar to those of B and Np. In glasses containing thorium, the thorium concentrated in the alteration phases.

Development of Low-Temperature Phosphate Glasses. In the electrometallurgical treatment of spent nuclear fuels, fission products and transuranic (TRU) elements accumulate in the molten LiCl-KCl electrolyte. These elements can be removed from the molten salt by ion exchange in zeolite. In the current process flowsheet, the spent zeolite is converted into a composite waste form consisting of the zeolite and borosilicate glass. This composite is fabricated by hot isostatic pressing. An alternative process that avoids the scaleup limitations of hot pressing incorporates the zeolite into a low-temperature phosphate glass to produce a ceramic waste form.

Zinc phosphate glasses, which have a low glass transition temperature in the range of 325 to 375°C, permit relatively low processing temperatures of about 450-700°C. The low process temperatures reduce losses of volatile metals (*e.g.*, ^{137}Cs , ^{99}Tc , Cd), and the zinc phosphate system can incorporate chloride salts at loading levels of 10-15%. Leaching tests of salt-loaded phosphate glass samples showed about the same losses of Cs, Na, K, and Li as salt-free glass. This material is a possible candidate for the disposal of fission-product and TRU elements in the electrometallurgical process for EBR-II fuel.

Critical Review and Testing of Natural Analogs. During the 1990s, CMT workers conducted a comprehensive critical review on the use of natural glasses as analogs for the long-term behavior of nuclear waste glasses. Parameters that affect the reactions between glass and repository groundwater include temperature, glass composition, radiation, and ratio of glass surface area to water volume. A review was also prepared on the status of glass-reaction modeling.

Obsidian, a rhyolitic glass, and tektite are naturally occurring glasses that have survived in nature for millions of years. Studies of their reactions with water vapor, started in the

1980s, were continued into the early 1990s to see if their behavior could offer insights into the long-term corrosion of nuclear waste glass in a geologic setting and the development of more corrosion-resistant glasses. Obsidian and tektite are enriched in silica and depleted in alkali metals and boron, relative to nuclear waste glasses.

The reactions of both obsidian and tektite with water vapor have a common mechanism—molecular water diffusion. The isothermal hydration rate of both depends on the intrinsic water content, even though tektite contains a very small amount of water, about 0.01%. Extrapolation of hydration rates of tektite to repository-relevant conditions resulted in much lower rates than those observed with nuclear waste glasses, indicating that water diffusion might not be the controlling reaction mechanism for nuclear waste glasses. However, at the lower repository temperatures that would occur over time as the nuclear waste cools, other possible reaction mechanisms, such as ion exchange or dissolution, may diminish, allowing water diffusion to emerge as the dominant long-term mechanism.

Natural obsidian and basalt were subjected to vapor hydration tests at 75°C and relative humidities of 95 and 100% for periods up to seven years. The results indicated that vapor hydration tests of a few years duration can replicate corrosion behavior over several thousand years in nature. This test method can be used to forecast the long-term behavior of nuclear waste glasses under similar conditions.

Immobilization of Plutonium in Glass. One of several alternatives under consideration by DOE for the long-term disposal of plutonium from dismantled nuclear weapons and cleanup of weapon production sites is fixation in a glass or ceramic. In a program begun in 1993, CMT investigators developed a low melting (1150°C) alkali-tin-silicate glass (ATS) for

immobilizing plutonium. This glass was engineered to accommodate a high plutonium loading (up to 7.0 wt% plutonium as PuO_2) together with gadolinium (as Gd_2O_3) added as a neutron absorber to mitigate against criticality problems during preparation, storage, and ultimate disposal of the glass. In ANL vapor-hydration tests, the durability of this glass was better than that of an Environmental Assessment reference glass. No significant reaction had occurred on exposure of the glass to water-saturated air at 200°C for 56 days.

Another glass that will be tested in the future is a lanthanide borosilicate glass that is also chemically durable and can dissolve substantial amounts of plutonium oxide, as well as the neutron absorbers, gadolinium and hafnium (as their oxides).

Argonne participated in the Fissile Materials Disposition Program by (1) characterizing a ceramic waste form being developed at Lawrence Livermore National Laboratory (LLNL), (2) corrosion testing of the LLNL ceramic, and (3) corrosion testing of plutonium-loaded glasses prepared at Savannah River, Pacific Northwest, and Argonne. The characterization study of the LLNL ceramic showed a number of titanate-based phases, and other types of phases such as perovskites and undissolved PuO_{2-x} . Both Pu(IV) and Pu(III) appeared to be present in a zirconolite phase. Titanate ceramic was selected as the waste form for the disposition of surplus plutonium. Advantages cited for the titanate ceramics are their ability to accept various cations as substitutes in their structure and their high resistance to aqueous corrosion.

Analytical Support. A sophisticated analytical capability was developed for analyzing the products of reactions of nuclear waste glasses with water and water vapor in a simulated Yucca Mountain Repository environment and for following their behavior (transformation, loss) with time. Applied were various

analytical techniques that fall under the general heading of analytical electron microscopy (AEM). These include transmission electron microscopy (TEM), X-ray energy dispersive spectroscopy (EDS), electron energy loss spectroscopy (EELS), and electron diffraction (ED). Point-to-point resolution of images approaching 3 Å could be achieved with TEM, 200 Å with EDS, and 20 Å with EELS and ED. Extremely thin samples, 500 Å or thinner, were required for these analyses. A specially designed diamond knife was effective in preparing ultrathin sections of a wide variety of reacted glasses.

Personnel. Many individuals, including temporary personnel, were involved in this program. Full-time CMT people included Teofilo Abrajano, Allen Bakel, John Bates, Dick Biwer, Charles Bradley, Edgar Buck, Jim Cunnane, Bill Ebert, Jeff Emery, Xiangdong Feng, Bob Finch, Tom Gerding, Joe Hoh, Jim Mazer, Denis Strachan, Shiu-Wing Tam, Stephen Wolf, Dave Wronkiewicz, and John Young.

TESTING OF SPENT FUEL

The reference design for limiting radionuclide release from spent UO_2 fuel stored in the proposed Yucca Mountain Repository is an engineered, multiple-barrier system surrounded by volcanic tuff. After long storage of the spent fuel in the repository (several hundred years), the barriers are breached, allowing exposure of the fuel material to the repository environment. Ongoing tests were started in the mid-1980s with both unirradiated and irradiated UO_2 (spent fuel) to compare their behavior and to determine the radionuclide release characteristics of the spent fuel in a water-unsaturated environment typical of that in the repository.

Unsaturated Tests with Unirradiated UO_2 . In these tests, Zircaloy-clad UO_2 pellets in a

stainless steel test vessel supported by a Teflon stand were exposed to water at 90°C dripping at a rate of 0.75 mL every 3.5 days. The water was a Nevada well water (EJ 13) that had been equilibrated with volcanic tuff of the repository. The release rate of the uranium was rapid for the first two years of exposure because of preferential corrosion along the grain boundaries and spallation of UO_2 grain particles from the sample surface (see Fig. 6-9). After two years, the UO_2 release rate decreased by an order of magnitude, remaining at a relatively constant value thereafter. This rate reduction was caused by the formation of a dense mat of uranium silicates that enveloped the loosened UO_2 grains at the sample surface. The uranium release rate ranged between 0.1 and 0.3 $\text{mg/m}^2\cdot\text{day}$. Most of the released uranium (86 to 97%) was sorbed on the walls of the stainless steel test vessel and the Teflon support stand. From 1 to 12% of the uranium was present in the leachate as >5-nm particles composed mainly of alkali or alkaline earth uranium silicates. Only about 2% of the uranium was dissolved in the leachate.

Tests with Irradiated UO_2 Spent Fuel. In these tests, small chunks (0.3 to 1 g) of irradiated fuel having a burnup of 30-40 $\text{MW}\cdot\text{day/kg U}$ were exposed to dripping

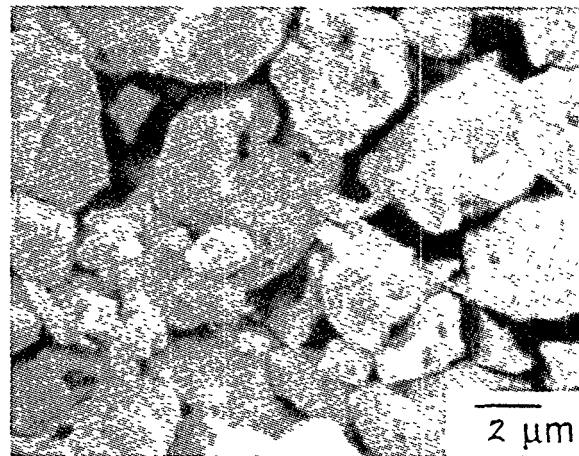


Fig. 6-9. Intergranular Corrosion and Spallation in UO_2 Samples

Nevada well water at 90°C. A layer of uranium silicates analogous to those found on unirradiated UO_2 formed on the surface. Over the first 580 days, a small fraction of the actinides (10^{-6} to 10^{-7}) was released to the leachate, appearing as dissolved species, colloids, and precipitated materials on the test vessel walls.

Of particular interest was the release of technetium (^{99}Tc), which did not change over a four-year test period and was more than 100 times greater than the release rate of uranium. The fraction of technetium released provides a lower limit for the extent of fuel reaction. Moreover, the constant rate of technetium release suggests that a surface reaction may be the rate-controlling step and that through-grain dissolution may dominate over grain-boundary-enhanced dissolution.

Drip tests of UO_2 have been in progress for over 13 years. Uranium release was rapid during the first two years, but the rates were lower in the following ten years. The rapid release was attributed to preferential corrosion along the UO_2 grain boundaries and spallation of very small (1 μm or less) UO_2 particles. After two years of reaction, a dense mat of U(VI) alteration phases had enveloped the UO_2 particles, decreasing the release rate.

Another test method called "petri-dish tests" was developed to measure the compositions of thin films of solutions in contact with the fuel specimens. The resulting data are used in model development and confirmation. Some information was obtained on the amounts of released plutonium and the percentage in colloidal form.

Personnel. Pat Finn played a major role in some of these activities. Others were Allen Bakel, John Bates, Edgar Buck, Dave Chamberlain, Jim Cunnane, Jeff Emery, Bob Finch, Tom Gerding, Lohman Hafenrichter, Joe Hoh, Susan Slater, Mark Surchik, Ben Tani, Ewald Veleckis, Stephen Wolf, and Dave Wronkiewicz.

WASTE ISOLATION PILOT PLANT PROJECT

In a program begun in 1989, CMT researchers investigated the effect of ionizing radiation on aspects of importance to the long-term performance of the Waste Isolation Pilot Plant (WIPP) repository. The work was part of an overall effort, coordinated by Sandia National Laboratories, to assess the performance of WIPP for long-term disposal of TRU waste. Measurements were made of the gas evolved over a 160-day test period from WIPP brine spiked with Pu(VI). Hydrogen was the primary gaseous product of radiolytic origin. Gas generation rates were 0.14, 0.002, and $<0.0003 \text{ mol}/(\text{m}^3\cdot\text{y})$ for Pu(VI) concentrations of 10^{-4} , 10^{-6} , and 10^{-8} M , respectively. Such data enable an assessment of the contribution of radiolytic gas generation to the overall gas generation rate in the repository. The ANL personnel in this project included Don Reed, Peter Lindahl, and Shigeo Okajima.

VITRIFICATION OF LOW-LEVEL WASTE

The safe disposal of radioactive and toxic waste elements requires durable waste forms that effectively isolate these components from the biosphere. In 1992, work was begun on vitrification for treatment and disposal of low-level and mixed wastes. Glass or glass/ceramic waste forms were sought for inexpensive remediation of contaminated materials, including soils, waste tank sludges, evaporator sludges, industrial catalysts, incinerator residues, High Efficiency Particulate Air (HEPA) filters, and equipment.

Development of Low-Level Glass Waste Forms. The objective of this work was to identify and produce glass formulations that could be used to vitrify low-level wastes such as those listed above. A composition envelope

was developed for satisfactorily incorporating these wastes in a range of alkali boroalumino-silicate glasses. Glasses within this envelope could be produced with relatively small (7 to 28%) additions of glass-forming materials, *e.g.*, borax, diatomaceous earth, boric acid, and sodium carbonate. The overall waste volume was reduced by a factor of four to eight, and the glasses so produced met EPA requirements. The work provided compelling evidence that a wide variety of ANL waste streams could be vitrified in borosilicate glasses.

Glass-Crystal Compositions. Many DOE sites have large volumes of radioactive waste that are not amenable to disposal in glass waste forms. These wastes contain large amounts of metallic elements such as Cr, Ni, Ti, Fe, Ca, and Mg, which have low solubilities in glass. Glass-crystal composite waste forms consisting of crystals encapsulated in a glass matrix were evaluated for their potential in disposal of these mixed low-level and hazardous waste materials. Crystal formation was induced from the melts by proper blending of the simulated waste streams, use of chemical additives such as Zr, Ti, and P, and slow cooling of the melts from the 1400°C melting temperature. Hazardous elements such as U, Pu, Sr, Cd, Pb, As, and Ba can be incorporated into corrosion-resistant crystalline phases. The glass-crystal composites were very resistant to aqueous corrosion. In fact, the uranium release rate from two composite samples was 100- and 300-fold lower than that from a Savannah River borosilicate glass, a result attributed mainly to the durability of the crystalline phases and to the durable nature of the glass matrix.

It was concluded that glass-crystal composites combine the excellent durability of predominantly crystalline waste forms, such as Synroc, with the ease of processing

offered by the use of commercially available vitrification facilities.

Testing of Glass Waste Forms for Low-Level Wastes. Several glasses developed at Pacific Northwest Laboratory as part of the Hanford low-level waste project were provided to ANL for testing. Three-year tests of two sodium-rich borosilicate glasses, designated LD6-5412 and FLLW-1, were begun in 1994. After the first two years, sodium release was higher than that of silicon or boron, and its release was by a diffusion-controlled, ion-exchange process. The formulation of alteration glasses on the surface of the LD6-5412 glass caused a dramatic increase in the dissolution rate of that glass. The alteration phases also affected the release of radionuclides present in the FLLW-1 glass. Final conclusions await the completion of the third year of tests.

Personnel. The vitrification work involved Allen Bakel, John Bates, Edgar Buck, Dave Chamberlain, Cliff Conner, Jim Cunnane, Bill Ebert, Adam Ellison, Jeff Emery, Xiangdong Feng, Bob Finch, Jeff Fortner, Jim Helt, Joe Hoh, Terry Johnson, Ted Krause, Jian Shu Luo, Jim Mazer, Carol Mertz, Luis Nuñez, Dale Smith, Denis Strachan, Ben Tani, Stephen Wolf, Dave Wronkiewicz, and Dave Wygmans.

CHARACTERIZATION OF CONTAMINATED SOILS AND OTHER MATERIALS

Analytical electron microscopy, described earlier, was brought to bear on the characterization of the following contaminated soils and materials to assist in the remediation of the sites.

Contaminated Soils at the Fernald Site. The Fernald site had become heavily contaminated with uranium as a result of uranium

processing operations. The major uranium-bearing phase in the soil was identified as a calcium uranyl phosphate. Also found in the soil were phosphate phases that resulted from the use of tributyl phosphate in the uranium purification process.

Johnson Atoll Soil. In the early 1960s, uranium and plutonium contamination of Johnson Atoll in the Pacific resulted from an abort of a nuclear weapon. Analyses of fragments of bomb components showed that plutonium and uranium in these fragments had oxidized and formed carbonate complexes, facilitating their migration to surrounding soils.

Rocky Flats Incinerator Residues. Plutonium in Rocky Flats incinerator residues was found to exist mainly in the form of a reduced oxide, PuO_{2-x} . Some plutonium was also incorporated into a silicate glass in the ash.

Cement Mortar Formulations. Leach tests were conducted on cement mortar formulations from Applied Innovation Inc., to evaluate their ability to retain radioactive elements from radioactive waste, as well as elements in toxic and mixed waste. According to the Nuclear Regulatory Commission, the effective diffusivity of an element in an acceptable low-level waste form should be less than 10^{-6} (leachability index of six). Leachability indices measured for Tc, Cs, Ni, U, Se, As, and Cd were 15, 14, 21, 22, 15, 18, and 18, respectively. These excellent results showed that Portland-cement mortars are promising for immobilizing these wastes.

Personnel. Various aspects of this work were carried out by John Bates, Edgar Buck, Dave Chamberlain, Mike Chen, Cliff Conner, Jim Cunnane, Jack Demirgian, Jeff Fortner, Jim Helt, Ted Krause, Don Reed, John Schneider, Ian Tasker, George Vandegrift, and Stephen Wolf.

OTHER PERSONNEL

Besides the people listed specifically in the above programs, the following also played an important role in the Nuclear Waste Management effort: John Basco, Mark Clark, Tom DiSanto, John Falkenberg, Margaret Goldberg, Mike Goss, Mark Hash, Joe Hoh, Terry Johnson, Mike Kaminski, Lester Morss, Mike Nole, Kevin Quigley, Wally Seefeldt, Chuck Seils, Dan Shull, and Sy Vogler. Secretaries were Lauren Ambrose, Norma Barrett, Elaine Estand, Susan McKinney, Sue Rura, and Virginia Strezo. Roberta Riel was in charge of quality assurance (QA).

Separation Science and Technology

One of the major programs in this area through the mid 1990s was the Transuranic Extraction (TRUEX) process for recovering TRU elements from a wide variety of aqueous systems and for lowering disposal costs of nuclear wastes. Three other solvent-extraction processes introduced in the 1990s for cleanup of nuclear wastes were the SREX (strontium extraction) and CSEX (cesium extraction) processes for removing strontium and cesium, and the NEPEX (neptunium-plutonium extraction process) for selectively partitioning Np(IV), plutonium, and uranium. These processes could be used in different combinations to achieve various recovery and separation objectives. Improvements continued to be made in ANL-designed centrifugal contactors for specific process applications.

Other programs were:

1. Concentration of plutonium solids in pyrochemical residues by aqueous biphasic extractions.
2. Membrane-assisted solvent extraction for treating natural and process wastes contaminated by volatile organic compounds.

3. Evaporation/concentration technology for concentrating radioactive waste and product streams.
4. A process for separating ^{99}Mo from low-enriched uranium targets for nuclear medicine uses.
5. Technical support to ANL management for treating transuranic and organic-containing wastes.

DEVELOPMENT AND APPLICATION OF TRUEX TECHNOLOGY

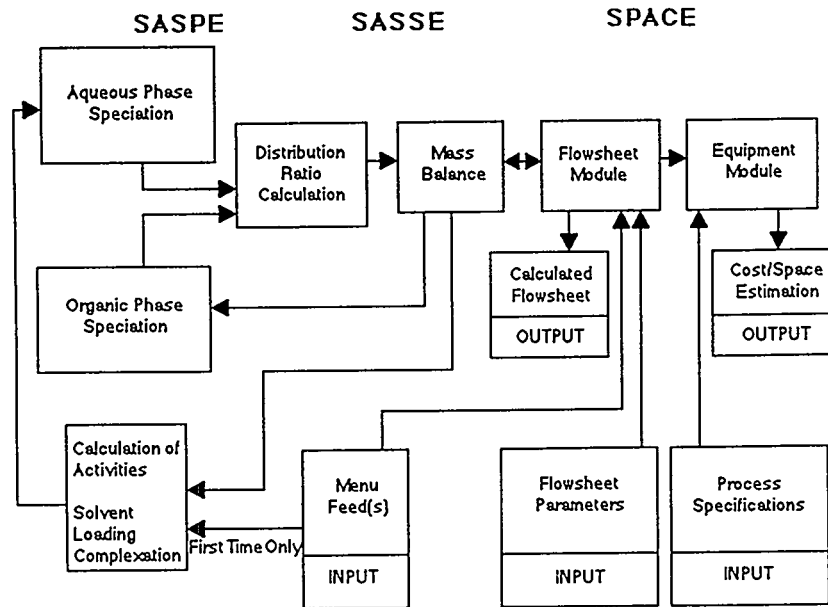
The TRUEX process was outlined in Chapter 5. The use of trichloroethylene or carbon tetrachloride as a diluent for the TRUEX extractant, CMPO [octyl(phenyl)-N,N-diisobutyl carbamoyl phosphine oxide], was discontinued because of growing environmental, safety, and health concerns. Instead, a normal paraffinic hydrocarbon (C_{12} - C_{14}) mixture or normal dodecane was used. Degradation of this solvent combination by hydrolysis and radiolysis was shown to be very low, the fraction of the CMPO decomposing in one year's operation (100 processing cycles) being only 8.6×10^{-4} .

Generic TRUEX Model. Improvements continued to be made in the Generic TRUEX Model, a computer program first issued in 1989 as a tool for (1) designing TRUEX flowsheets for specific waste stream compositions, process constraints, and goals; (2) estimating space and cost requirements for installing the TRUEX process; and (3) monitoring and controlling the process. These functions were performed by executing different modules within a computer code, illustrated in Fig. 6-10. The success of the GTM was dependent on underlying data that were sound, correct, and defensible. A data base for generating the code, which was begun in 1987, consists of information from the literature, laboratory results from CMT,

and information on the extraction behavior of all important feed components over a wide range of possible waste-stream and processing compositions. An operating manual for the generic TRUEX process was prepared by Scott Aase, Dave Chaiko, Lorac Chow, Dave Chamberlain, Jaqueline Copple, Don Fredrickson, Ray Jaskot, Ralph Leonard, Luis Nuñez, Monica Regalbutto, Jake Sedlet, Ian Tasker, Verne Trevorrow, George Vandegrift, and Erv Van Deventer. Updated versions of the Generic TRUEX Model were published annually through 1994 to incorporate new information and capabilities that were introduced. Development of the TRUEX process was terminated at the end of September 1995.

Validation of the Generic TRUEX Model. When there was the opportunity, the GTM was tested experimentally. One opportunity was the processing of analytical wastes from the New Brunswick Laboratory, using a flowsheet and equipment of a GTM design. The TRU content of the raffinate was 1.8 nCi/mL, a reduction of 22,000 from the concentration in the feed. The calculated raffinate concentration using the GTM was 1.0 nCi/mL. This remarkable agreement provided confidence in using the GTM for designing flowsheets and equipment for processing the much larger volumes of TRU wastes generated at the Rocky Flats Plant, Los Alamos National Laboratory, Hanford, and the Idaho Chemical Processing Plant.

Treatment of New Brunswick Laboratory Analytical Wastes. Over 200 L of waste solution from the analysis of plutonium samples had accumulated at the New Brunswick Laboratory and at Argonne. The Chemical Technology Division was given the project of converting the bulk of this material into a non-TRU (low-level) waste. The design of a flowsheet and equipment was based on



SASSE = Spreadsheet Algorithm for Stagewise Solvent Extraction
 SASPE = Spreadsheet Algorithm for Speciation and Partitioning Equilibria
 SPACE = Spreadsheet for Calculating Equipment Size, Plant Space, and Capital Costs

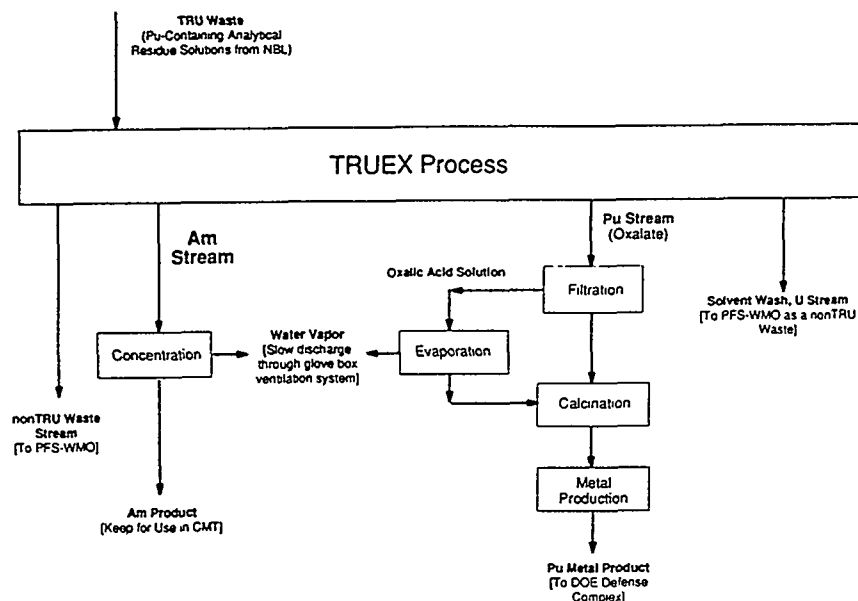
Fig. 6-10. Interactions among Computer Program Modules of the Generic TRUEX Model for Flowsheet Calculations

an initial goal of less than 10 nCi/mL of TRU in the low-level waste. The flowsheet for this operation is shown in Fig. 6-11.

The TRUEX process was conducted in a 20-stage centrifugal contactor bank (4-cm-dia rotors) installed in a glove box. Six stages were devoted to extraction, two to scrubbing, six to stripping americium, four to stripping plutonium, and two to washing the solvent to remove degradation products and permit recycle of the solvent. The goal of 10 nCi/mL or less of TRU activity was easily achieved, but after the first batch of New Brunswick waste solution had been processed, the ANL Waste Management Operation changed the goal from 10 nCi/mL to 0.1 nCi/mL or less, a reduction of 100 from the original goal. Achieving this very low TRU concentration in the waste would have necessitated radical changes in the flowsheet. It was decided to finish the campaign, using the original

flowsheet. Raffinate TRU concentrations of 10 nCi/mL or less (generally between 2 and 5 nCi/mL) were achieved in processing the remaining batches. Note that these concentrations are well below the 100 nCi/mL of TRU below which solutions are classified as non-TRU, allowing them to be treated as low-level waste.

Demonstration of SREX Process. The SREX (strontium extraction) version of the TRUEX process was selected as the reference process for the removal of strontium from high-level sodium-bearing and calcined wastes produced at the Idaho Chemical Processing Plant. The process was invented by researchers in the ANL Chemistry Division, and the CMT Division provided engineering and modeling support, including design, fabrication, and testing of a 24-stage "minicontactor" to be used for a process demonstration at Idaho



A bank of 20 centrifugal contactors with 4-cm-dia rotors was employed, six for extraction, two for scrubbing the solvent extract, six for extracting americium, four for extracting plutonium, and two for washing the solvent. Conversion of the plutonium to metal by precipitation of the oxalate, calcination of the oxalate to yield PuO_2 , and reduction of the PuO_2 to metal was not performed.

Fig. 6-11. General Flowsheet for Processing Plutonium Waste Solutions of New Brunswick Laboratory

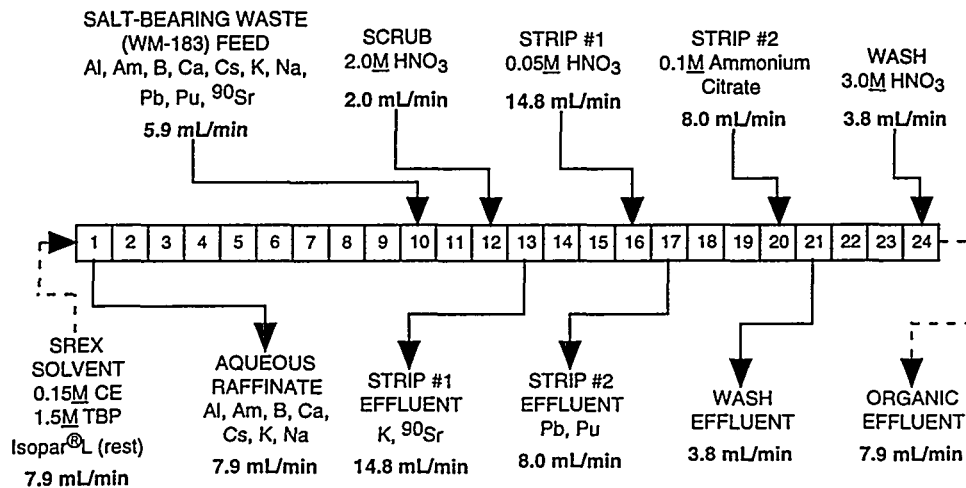
National Engineering and Environmental Laboratory (INEEL). The flowsheet is shown schematically in Fig. 6-12.

The hot demonstration of the SREX process at INEEL went very smoothly, with 99.995% of the ^{90}Sr being removed from the aqueous raffinate. With this removal efficiency, the ^{90}Sr activity was decreased to 0.0089 Ci/m^3 , which is well below the limit for low-level waste.

Demonstration of SRTALK Process. A collaborative program was undertaken with Oak Ridge and Pacific Northwest National Laboratories on the SRTALK (Sr, Tc, and Cs alkaline-side extraction) process. This is a solvent-extraction process that can separate alkali-metal pertechnetate salts from the alkaline supernate that comes directly from

nuclear waste-storage tanks. Two advantages of the SRTALK process over the ion-exchange columns currently used for this purpose are (1) the technetium is recovered free of other salts in the tank supernate, and (2) no added chemicals (*e.g.*, tin, ethylene diamine) are required to strip technetium from ion-exchange columns. These features would reduce greatly the number of glass canisters needed for waste disposal.

The SRTALK solvent consists of 0.04 *M* crown ether and 1.8 *M* tributyl phosphate in Isopar[®]L, which extracts technetium from the feed with a distribution ratio of 6 to 10, and can be stripped of technetium with water or dilute nitric acid. The process concept was demonstrated first in a test tube, then in a minicontactor. The final flowsheet is shown in Fig. 6-13.



The tests were conducted in a shielded cell at ICPP in Idaho. The SREX solvent was a crown ether and tributyl phosphate in Isopar[®]L. The ⁹⁰Sr in the sodium-bearing waste feed was removed by the solvent in the extraction section (stages 1-10). Other components in the feed were washed back by the scrub feed in stages 11 and 12. In the first strip section (stages 13-16), dilute acid stripped ⁹⁵Sr and any potassium out of the solvent. In the second strip section (stages 17-20), a complexing agent (ammonium citrate) stripped lead and actinides from the solvent. The solvent was reacidified in stages 21-24 so it could be recycled to stage 1.

Fig. 6-12. Flowsheet for a Test of the SREX Process with Hot Tank Waste at INEEL

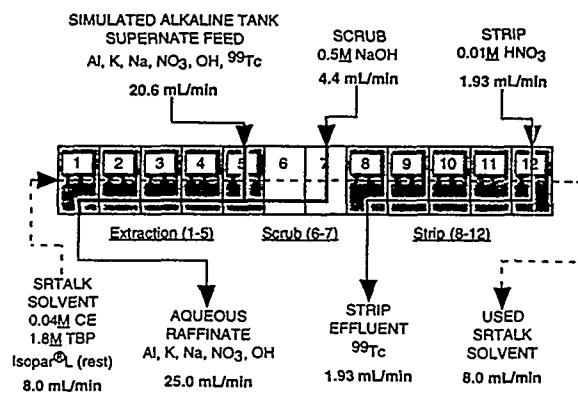
Tests of the SRTALK process were very successful, and plans were made to extend the process to Cs and possibly Sr extractability.

CENTRIFUGAL CONTACTOR DEVELOPMENT

Ralph Leonard continued to adapt the basic design of the centrifugal contactor to various applications by use of computer models for (1) the flow of organic and aqueous phases through the contactor and (2) the vibrational parameters of the spinning motor/rotor combinations. By use of these models, a new contactor design was developed that, without increasing rotor diameter, would double the throughput. The high throughput design was developed for use in the proposed PUREX facility at the Hanford Plutonium Finishing Plant.

This work was later extended to the design of a super high-throughput centrifugal contactor that would increase the throughput by a factor of four to eight, yet keep the unit criticality safe by use of rotor diameters of less than 10 cm. Thus, a single bank of contactors could handle a throughput that otherwise would have required four to eight banks of contactors. Figure 6-14 is a schematic drawing of a two-stage super high-throughput contactor.

Twelve-stage banks of contactors were built for Pacific Northwest Laboratories and the Lockheed Idaho Technology Co. so that they could carry out pilot-plant tests of solvent-extraction processes for cleaning up their nuclear wastes. An ANL-type contactor fabricated of Kynar[®], which has high resistance to attack by HCl, was designed for removal of plutonium and uranium from Los Alamos chloride salt wastes.



In stages 1-5, the technetium is extracted into the organic phase and a scrub section in stages 6 and 7 is used to free the tank solution of other salts. In stages 6-12, the technetium is back-extracted into a 0.01 M nitric acid solution. The strip effluent is essentially free of added chemicals. By suitable adjustments of the organic-to-aqueous flow ratios in the extraction and strip sections, the technetium concentration in the strip effluent can be increased by a factor of 10 compared to that of the aqueous feed. At the same time, the decontamination factor for technetium in the aqueous raffinate can be kept over 6.4, as required.

Fig. 6-13. Flowsheet for SRTALK Demonstration

Hydraulic and vibrational analyses were also used to assist in the design of a high-temperature (500-800°C) centrifugal contactor for contacting molten chloride salt wastes (produced in the electrometallurgical process) with liquid cadmium to extract plutonium (see Chapter 5).

An outgrowth of the centrifugal contactor development was a concept for a continuous countercurrent solid-liquid contactor for mixing and then separating liquid and solid phases. Such a contactor could be used for washing sludges from the Hanford and Savannah River waste tanks to, in the case of the Savannah River sludges, remove selected

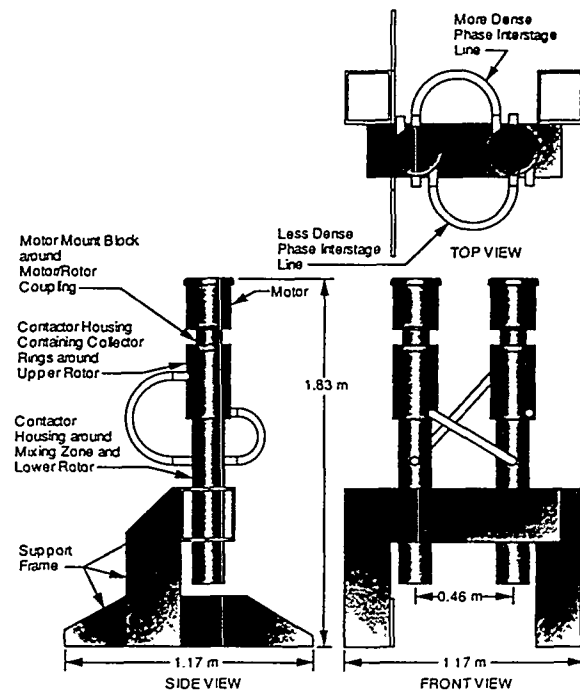


Fig. 6-14. Two-Stage Super High-Throughput Centrifugal Contactor

constituents such as cesium and strontium. Figure 6-15 shows two stages of a solid-liquid contactor. Solid particles, which have a higher energy density than the liquid, move by gravity, countercurrent to the liquid flow.

Ralph Leonard was the leader of the work on centrifugal contactors. Others who participated in this work were Dave Chamberlain, Cliff Conner, Monica Regalbuto, George Vandegrift, and Dave Wygmans. The high-temperature molten salt contactors were developed primarily by Terry Johnson with John Ackerman, John Basco, and Lorac Chow.

RECOVERY AND SEPARATION OF MOLYBDENUM-99

Work on the extraction of ⁹⁹Mo from low-enriched uranium (LEU), which was begun in 1985 by George Vandegrift, was resumed in 1993 after a dormant period of four years.

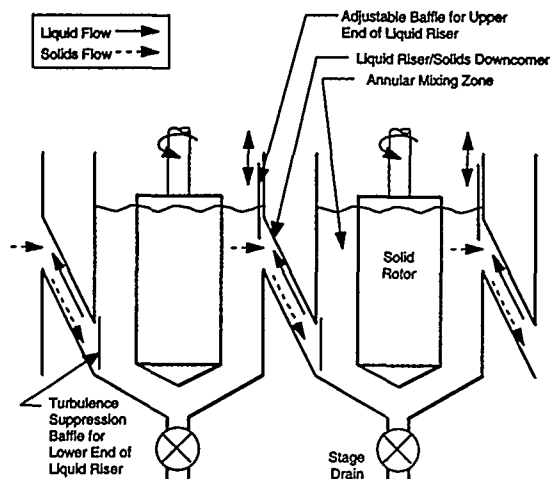


Fig. 6-15. Two Stages in Continuous Countercurrent Solid-Liquid Contactor

This four-year hiatus resulted from low budgets for the program on Reduced Enrichment for Research and Test Reactors (RERTR) from which the CMT program obtained its funding. Revival of the program was prompted by 1993 legislation that severely restricted the export of high-enriched uranium (HEU) and placed emphasis on the use of LEU.

To overcome the low-concentration of ^{235}U in LEU, while maintaining the same target geometries, targets having high concentrations of uranium were sought. Uranium silicide (U_3Si_2) and uranium metal foil were proposed as substitutes for the HEU target materials previously used (UAl_x and a thin layer of UO_2 on the inside of a cylindrical target). After they are irradiated, the target materials must be dissolved, after which molybdenum is precipitated quantitatively from the solution by alpha-benzoin oxime ($\alpha\text{-BO}$). Purified molybdenum containing the ^{99}Mo isotope is deposited on a column of alumina, from which its decay daughter, metastable technetium-99 ($^{99\text{m}}\text{Tc}$), may be eluted periodically with a saline solution. The $^{99\text{m}}\text{Tc}$, which has a half-life of 6.02 h, is used in medical diagnoses.

The CMT program was focused on target designs for the two LEU target materials and

on methods of dissolving the irradiated targets. Because irradiated targets were processed in other countries (Indonesia, Argentina, and South Africa), CMT developments were designed for application in those facilities.

Use of uranium foil was found to require thin metal barriers to prevent bonding with the target container material. Barriers of iron, copper, and nickel about 10- μm thick performed well.

In the Cintichem process used in Indonesia, a 3 M H_2SO_4 -2 M HNO_3 solution was used to dissolve irradiated UO_2 targets. While this acid mixture could also be used to dissolve uranium metal foil and metal barriers of copper, nickel, or iron, the presence of sulfate in the acidic waste solution complicated the uranium recovery, volume reduction, and waste disposal. The CMT researchers found that dissolution of uranium foil and any barrier materials could be accomplished at the same rate in 8 M HNO_3 . Elimination of sulfuric acid did not significantly affect the recovery of molybdenum by precipitation with $\alpha\text{-BO}$ or the purity of the final product.

Dissolution of uranium foils with alkaline peroxide (e.g., 5 M H_2O_2 -1.5 M NaOH) was investigated as a replacement for processing HEU aluminate targets. Unfortunately, the uranium surface catalyzes the destruction of H_2O_2 , resulting in the consumption of a very large amount of peroxide. By sequential small additions of peroxide, the consumption was reduced 20 fold (from 100 to 5 times the stoichiometric amount required for dissolution). The barrier metal candidates of copper, nickel, and iron are not dissolved by the peroxide solution. For this situation, investigations of other barrier materials, such as zinc, were started.

Although dissolution of uranium silicide, proposed as an alternative to uranium aluminate, was investigated, work on it was suspended due to difficulties in dissolving the silicide, problems caused by dissolved silicate

in recovery of the molybdenum, and the relatively high degree of success achieved with uranium foil targets.

The current studies are aimed at development of a process for separating molybdenum from LEU (and its fission and absorption products) that is as similar as possible to the Cintichem process used in Indonesia with highly enriched uranium. Two LEU target designs, uranium metal foil and UO_2/Al dispersion fuel, are being investigated. The CMT work in this area consisted of three major areas: (1) the behavior of fission products (I, Rh, and Ag) in the Cintichem process, (2) the effects of zinc fission barriers for uranium-foil targets, and (3) a procedure that will measure alpha contamination in the ^{99}Mo product.

The investigators concluded that contamination of the molybdenum product by the three fission products would not be a problem. An effort was mounted on a procedure for separating and recovering ^{99}Mo that will allow low-dose, facile, and effective measurement of alpha contamination in the ^{99}Mo . In the development of metal-foil targets, the use of thin metal barriers (to fission recoil) between the uranium foil and the target walls was investigated, zinc being a major contender. Studies were also conducted on the use of alkaline peroxide solutions for dissolution of UO_2 and metal foil targets.

This work, led by George Vandegrift, was done by Scott Aase, Cliff Conner, Joe Hutter, Jane Kwok, Ralph Leonard, Samson Marshall, Jake Sedlet, "Chino" Srinivasan, Don Vissers, and Dave Wygmans.

MISCELLANEOUS PROGRAMS

In the area of Separation Science and Technology, a number of other small programs of varying duration were conducted in the 1990s. They are the following.

1. Aqueous biphasic extraction in which colloid-size particles partition between two immiscible aqueous phases. A possible application is the separation of ultra-fine PuO_2 particles from other materials.
2. Separation of volatile organic compounds from groundwater by means of membrane-assisted solvent extraction in which the organics are transferred through a porous membrane to an extractant such as sunflower oil.
3. An advanced evaporator technology for concentrating radioactive waste and product streams and for achieving very high decontamination factors in the condensate (in the range of 10^6 to 10^7). To advance this technology, CMT procured a laboratory-scale evaporator from LICON Inc., the design of which showed promise of achieving the requisite high decontamination factors.
4. Magnetically assisted chemical separation, which combines the selective separation afforded by chemical sorption with the physical separation provided by magnetic recovery of ferromagnetic particles. This work was aimed at separating cesium, strontium, and TRU elements from the waste tank sludges and supernatants in underground storage tanks at Hanford.
5. A closed-loop off-gas system that will prevent the direct release of toxic gases during incineration or vitrification of hazardous and mixed radioactive wastes.
6. The *in situ* decontamination of equipment (e.g., piping systems and storage tanks) in production plants.
7. Technical support to ANL Waste Management in the treatment of nuclear wastes for disposal, treatment of mixed wastes that contain hazardous metals (Pb, Cd, Cr, Ag, and Hg), and evaporator technology.

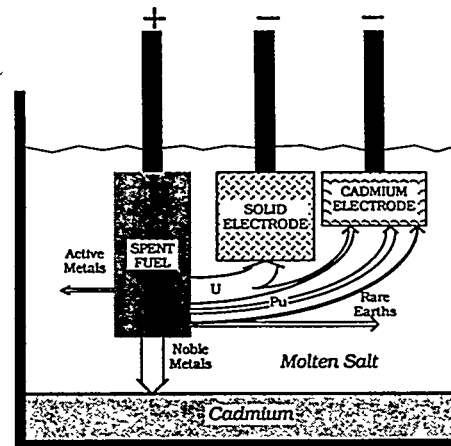
Integral Fast Reactor Pyrochemical Process

Work on development of a pyrochemical process for recovering and purifying fuel discharged from the proposed Integral Fast Reactor (IFR) continued until October 1995, at which time the IFR program was terminated.

PROCESS FLOWSHEET AND CHEMISTRY STUDIES

The evolution of the IFR pyrochemical process was described earlier in Chapter 5. In the process, shown schematically in Fig. 6-16, spent fuel in stainless steel cladding is chopped and dissolved anodically in molten LiCl-KCl at 500°C. During the dissolution, the uranium is electrotransported to solid cathodes. The plutonium and some uranium are then electrotransported to a liquid cadmium cathode. More than 99.9% of the actinides are removed from the cladding shells. The noble metal fission products either remain in the basket or fall as a particulate metal into the cadmium pool at the bottom of the electrorefiner. The alkali and alkaline earth metals in the spent fuel are converted to their chlorides and remain in the electrorefiner salt, as do most of the rare-earth fission products. Figure 6-17 is an artist's rendering of a commercial-scale facility.

Computer Code. A computer code, PYRO, which was developed by John Ackerman, accurately predicts the distribution of the elements in the electrorefiner during the individual operations of the process. This code was used extensively to calculate the compositions of product and waste streams under various conditions and to study fuel and waste processing strategies.



Quarter-inch-long segments of IFR core fuel are loaded into a porous stainless steel basket, which is suspended in the molten LiCl-KCl electrolyte at 500°C. Application of a dc voltage causes uranium to transport to a solid iron mandrel. Plutonium and the other transuranic elements and the alkaline earth, rare earth, and iodine fission products report to the electrolyte salt phase. Noble metal fission products remain either in the anode basket or are collected in the liquid cadmium pool at the bottom of the electrochemical cell. Gaseous fission products are released to the cell cover gas, from which they are removed for concentration and storage. Plutonium and other transuranic elements are subsequently transported to a liquid cadmium cathode along with some uranium and 10-20% of the rare earth elements. Contamination of the plutonium by rare earth elements provides a very strong deterrent to diversion of the plutonium for weapons use. The uranium and plutonium products are recovered by retorting to vaporize cadmium and drive off adhering electrolyte salt.

Fig. 6-16. Electrorefining Cell for IFR Pyroprocess

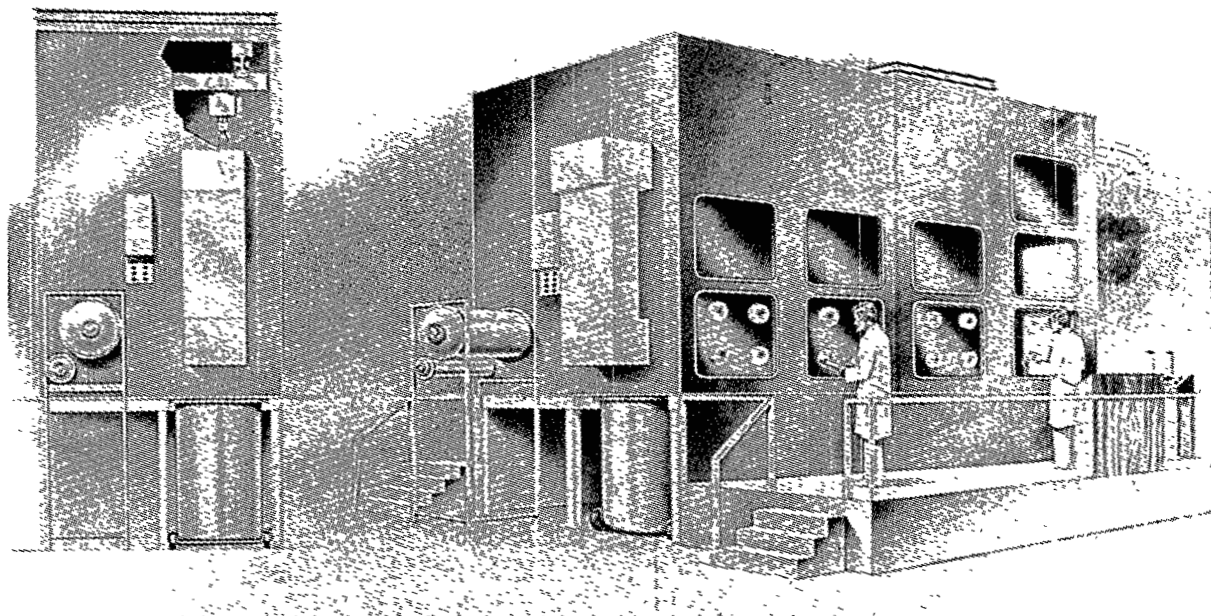


Fig. 6-17. Drawing of Commercial-Scale Facility for Processing of Spent Metal Fuel

Separation Factors. Part of the supporting chemistry studies for verifying the code were measurements of separation factors, which are the ratios of distribution coefficients of pairs of elements. The distribution coefficient of an element is its concentration in the salt phase divided by its concentration in the metal phase. Separation factors are useful in predicting salt and metal compositions, decontamination factors for impurity elements in the uranium and plutonium products, and the potential of countercurrent operations to amplify separations of various elements. Tables 6-7 and 6-8 give separation factors for several actinides and rare earth elements between cadmium and the LiCl-KCl molten salt electrolyte and an alkaline earth-rich salt used in the early process development. The latter salt was of the nominal composition (in wt%) 35 BaCl₂, 32 CaCl₂, 23 LiCl, and 10 NaCl. The rare earths, europium and samarium, behaved like the divalent alkaline earths, barium and strontium. These elements remained almost entirely in the salt phase. As

shown by the separation for the Y-La and Y-Nd pairs, yttrium was also more easily oxidized than were the rare earth elements. Jack Settle did this work under the direction of John Ackerman.

PROCESS DEVELOPMENT STUDIES

Salt/Atmosphere Reactions. For safety purposes, it was important to determine the consequences of a hypothetical accident that would result from inleakage of argon cell gas containing oxygen and water at concentrations up to 100 ppm into an electrorefiner. Ziggy Tomczuk and Bill Miller conducted some experiments to investigate this matter. On admission of the impure argon gas into an electrorefiner crucible, uranium was preferentially oxidized to UO₂, its concentration decreasing much more rapidly than that of plutonium. The finding that plutonium was not preferentially concentrated in the precipitate eliminated concern that a situation favorable to nuclear criticality would occur.

Table 6-7. Mean Separation Factors at 500°C

Element	Separation Factor ^a	
	LiCl-KCl Salt	Alkaline Earth-Rich Salt
Neptunium	2.12 ± 0.42	-
Plutonium	1.88 ± 0.09	1.32 ± 0.14
Americium	3.08 ± 0.78	2.85 ± 0.98
Curium	3.52 ± 0.59	2.3 ± 1.2
Cerium	45 ± 6	48 ± 13
Neodymium	39 ± 6	33 ± 5

^a Relative to uranium. Quoted uncertainty is standard deviation of the sample population.

Table 6-8. Measured Separation Factors for Pairs of Elements at 500°C

Element Pair	Separation Factor ^a	Element Pair	Separation Factor ^a
Nd-Pu	23.4 ± 1.2	Dy-La	3.79 ± 1.41
Am-Pu	1.54 ± 0.15	La-Ce	2.72 ± 0.37
Nd-Am	15.5 ± 1.1	La-Nd	3.01 ± 0.71
Nd-Pr	1.02 ± 0.04	Y-La	42.5 ± 9.3
Gd-La	1.10 ± 0.33	Y-Nd	140 ± 21

^a Quoted uncertainty is twice the standard deviation of the mean.

Corrosion Behavior of Steel Electrorefiner Container. After four years of operation at 500°C and continuous exposure to the electrolyte and cadmium phases of the electrorefining process, the low-carbon steel electrorefining crucible was destructively examined. There was no detectable corrosion of the vessel in either the salt- or cadmium-wetted areas, although, in the cadmium-wetted area, there was a thin U-Fe layer about 1-3 μm thick. No grain-boundary attack was evident. Low-carbon steel was concluded to

be an excellent material of construction for the electrorefining operation.

Zirconium Behavior. Zirconium constitutes about 30 vol% of IFR fuel. During electrorefining, most of it remained in the anode basket, but some of it escaped as particulate metal and was collected in the cadmium pool. At high voltages (0.5-0.7 V), some of it electrotransported with the uranium.

After 2.5 years of operation, a total of 11 kg of zirconium had been charged to the engineering-scale electrorefiner. Of this, about 3 kg had been removed in the uranium cathode deposits. (In the engineering-scale electrorefiner, uranium was electrotransported from the cadmium pool to an iron mandrel cathode.) About 0.5 kg of zirconium was in solution in the cadmium pool, leaving about 7.5 kg elsewhere in the electrorefiner. Samples of the cadmium pool showed no zirconium in suspension, nor was it vaporized as $ZrCl_4$ and deposited on the upper surfaces of the electrorefiner. Further searching revealed that it had deposited as $ZrCd_2$ on cadmium-wetted metal surfaces (principally the electrorefiner walls) near the salt-cadmium interface. This work was done by Erv Carls with the assistance of the electrorefiner staff—Eddie Gay, Nick Quattropani, and Jack Arntzen.

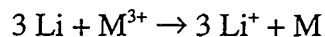
Removal of the zirconium by electrotransport requires that any uranium and plutonium dissolved in the cadmium be oxidized to their chlorides and transferred to the electrolyte. When this was done, zirconium was electrotransported to the iron mandrel cathode with the $ZrCd_2$ decomposing as the electrotransport proceeded.

The co-transport of uranium and zirconium to the solid cathode mandrel was also demonstrated. At low voltages (0.2 to 0.3 V), co-transport of zirconium with uranium was negligible, but at high voltages (0.5 to 0.7 V), the rate of zirconium transport with uranium was appreciable, and essentially complete transport of the zirconium could be achieved. This procedure has the advantage of direct recycle of zirconium for fabrication of new fuel.

Uranium-Plutonium Drawdown Procedure.

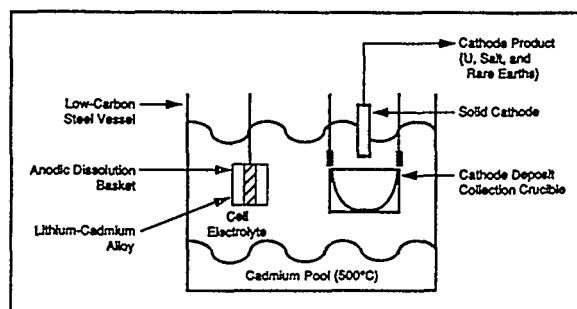
A uranium-plutonium drawdown procedure was required to remove these and other actinide elements from the electrolyte salt before it was removed to waste for further

processing. The drawdown procedure consisted of loading 5.8 wt% Li-94.2 wt% Cd (a solid) into an anode basket and, by ion displacement, transporting uranium to a solid cathode and uranium and plutonium to a liquid cadmium cathode. The reaction is



where M is uranium or plutonium. The net effect is to displace M^{3+} ions by Li^+ ions. A schematic representation of the drawdown procedure is shown in Fig. 6-18. The crucible below the cathode caught the deposits that slipped off the cathode.

In a series of eight drawdown runs, the uranium concentration in the electrolyte was reduced from 6.7 to 0.01 wt%. By the final run, 99.9% of the uranium had been removed along with only 13% of the rare earths. As the ion-displacement process continued, it was possible to reduce the rare earth concentration to less than 0.01 wt%.



In the uranium-plutonium drawdown procedure, a solid lithium-cadmium alloy (5.8 wt% Li-94.2 wt% Cd) is used as an anode. Under an applied voltage, lithium displaces uranium and plutonium in the salt. The crucible below the cathode is used to catch uranium that slips off the cathode. Plutonium is transferred to a liquid cadmium cathode. Usually, uranium and plutonium are deposited at different times, but in theory uranium and plutonium depositions could be made at the same time.

Fig. 6-18. Schematic Representation of Electrorefiner Drawdown

The feasibility of drawing down the PuCl_3 concentration by electrotransport of plutonium to a liquid cadmium cathode was also demonstrated in five scouting runs.

Electrotransport of Plutonium to Liquid Cadmium Cathodes. Work was done in the laboratory-scale electrorefiner to demonstrate the transport of plutonium to a liquid cadmium cathode. Some uranium was also electrotransported along with the plutonium. A problem with this operation was the growth of uranium dendrites from the surface of the cadmium once it became saturated with uranium. In uranium-saturated cadmium, the uranium has a chemical activity of unity, the same as that of uranium metal. If the uranium dendrites come in contact with the structure supporting the cadmium cathode, the cell short-circuits, and the transport of uranium and plutonium ceases.

The solid phase in equilibrium with plutonium-saturated cadmium is PuCd_6 , and, if the liquid cadmium cathode was to be of a reasonable size, the plutonium had to be "pumped" into the cathode until a large amount of PuCd_6 had been formed. The goal was a plutonium concentration of 10 wt% in the final product.

To eliminate the growth of uranium dendrites, a "pounder" was designed by Bill Miller (Fig. 6-19) to break up and push emerging dendrites back into the cadmium. The pounder was a cylindrical ceramic insulator (1/2-in. thick) that fit loosely within the crucible containing the cadmium. It was moved up and down and rotated around the cathode electrical lead to a new position for each up-and-down cycle. A wedge-shaped notch provided access to the salt electrolyte, which was pumped in and out of the volume between the cadmium surface and the upper position of the pounder.

Forty runs were made by Bill Miller, Ziggy Tomczuk, and John Heiberger to investigate

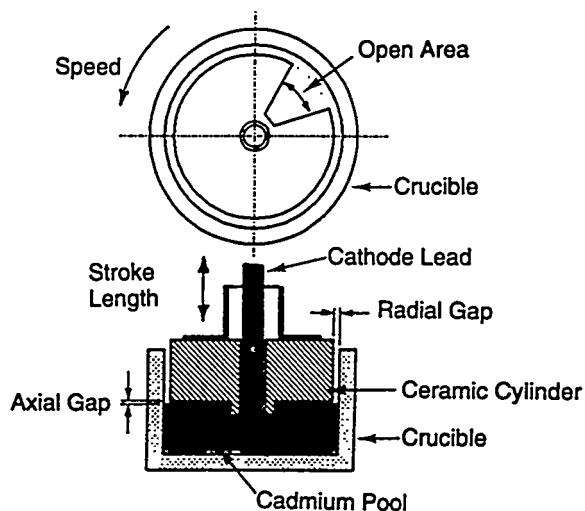


Fig. 6-19. Pounder Design for Liquid Cadmium Cathode

variables that might affect pounder performance, such as thickness of the radial gap, stroke length and frequency, spacing between the cadmium surface and the pounder at the low point of its stroke, rotation speed, transport current, and the ratio of plutonium to uranium in the electrolyte salt. Combinations of these variables were found that consistently controlled dendrite growth and prevented electrical short-circuiting.

In laboratory runs employing a 5-cm-dia ceramic crucible containing about 200 g of cadmium, collection efficiencies for uranium and plutonium were excellent, ranging between 95 and 100%. Figure 6-20 shows a typical product ingot. The goal of 10% heavy metal (U plus Pu) in the product was achieved routinely. The highest loading was 19 wt% (16 wt% Pu, 3 wt% U). Ceramic crucibles of either beryllia (BeO) or high purity AlN (no Al_2O_3) are not wetted by the cadmium and, when provided with a 4° taper, permit good release of the product ingots.

Retention of Noble Metals in Anode Baskets.

Tests using simulated EBR-II fuel were run to determine whether metal screens (200 or 325 mesh stainless steel) were needed in

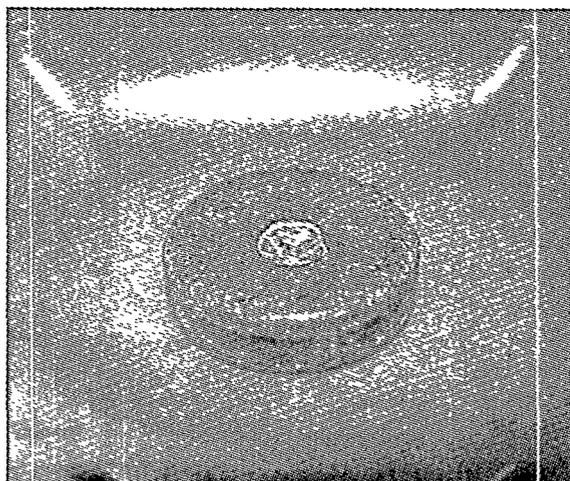


Fig. 6-20. Product Ingot of Deposit from Liquid Cadmium Cathode

anode baskets to retain the noble metals. These tests showed that 100% of the zirconium, 99% of the molybdenum, 60% of the palladium, 100% of the rhodium, and 92% of the ruthenium were retained in the anode baskets, whether or not screen retainers were employed. On average, 92% of the noble metal content was retained in the anode baskets. Yet to be determined is the retention of noble metals when actual spent fuel is processed. The minor fission products, selenium, antimony, and tellurium, were found to behave like the noble metals and, therefore, are also likely to be left in the anode baskets on electrotransport of the uranium.

Process Instrumentation. In the early 1990s, Jim Willit developed voltammetric techniques for measuring *in situ* the concentrations of uranium, plutonium, and rare earths in the electrolyte. In electrotransport of plutonium to the cadmium cathode, monitoring of the electrolyte composition is critical for controlling the composition of the cathode product. *In situ* concentration measurements were also very useful in following the concentrations of uranium and plutonium during drawdown operations.

Making such *in situ* measurements possible was the development of a reference electrode

based on the use of a sparingly soluble salt, K_xZrCl_{x+2} where x equals 1 or 2. A single-probe design that incorporated two reference electrodes, as well as working and counter electrodes, was developed. In all voltammetric techniques, a potential waveform is applied to the working electrode and the resulting current is measured. Current peaks occur at different voltages for the various elements. The size of the peak for a particular element is proportional to its concentration in the electrolyte. An investigation of waveforms disclosed that square-wave voltammetry was the preferred technique.

ENGINEERING-SCALE PROCESS DEVELOPMENT

Electrotransport of Uranium. Improved performance was achieved in the electrotransport of uranium from the cadmium pool to the single iron mandrel cathode. With mixing of the electrolyte discontinued during the latter portion of the two electrotransports, 9.5 and 9.3 kg of uranium were transferred in 37 and 26.5 h, respectively. Figure 6-21 shows one of the uranium deposits.

Dissolution of Spent Fuel. Anodic dissolution of U-Zr-fissium fuel pins was demonstrated at the plant scale (10 kg of uranium). With a coulombic efficiency of 50%, 99.8% of the fuel was removed from the cladding. Uranium was simultaneously deposited on a solid iron cathode. Anodic dissolution was concluded to be a practical operation for plant-scale application.

Equipment Testing. Harvesting of the uranium cathode deposit was achieved by pulling the iron mandrel through a die and collecting the stripped uranium in a steel basket. Three devices were tested for providing the stripping force—a torque wrench, an impact wrench, and a modified pipe threader. Good performance was realized

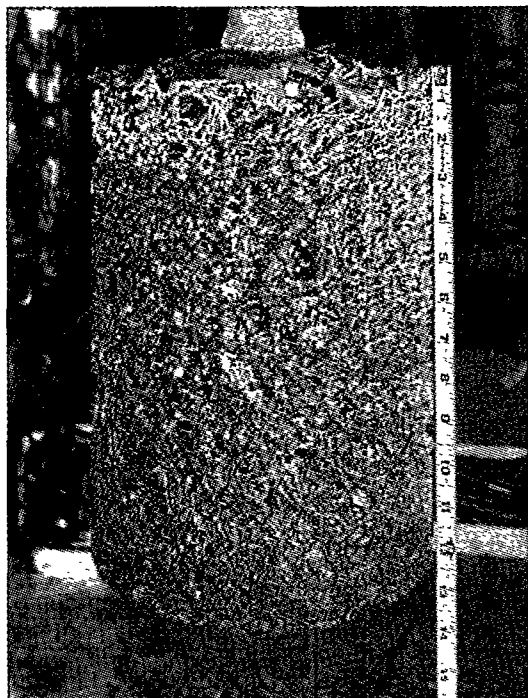


Fig. 6-21. Uranium Deposit (9.3 kg) on Single Mandrel Cathode

with the torque wrench and the modified pipe threader.

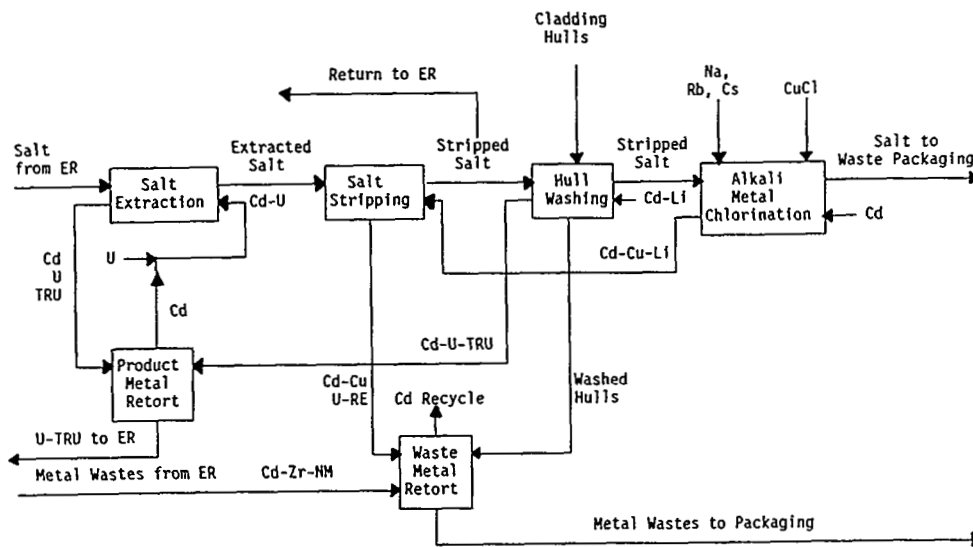
Cover Gas Treatment System. During operation of the engineering-scale electrorefiner, cadmium aerosols were released from the electrorefiner and deposited on the interior of the glove-box windows and on the equipment. Such deposition of cadmium could not be tolerated in the EBR-II Fuel Cycle Facility. To reduce the release of cadmium from the electrorefiner, a treatment system was designed for removal of cadmium vapor from the cover gas of the electrorefiner. The cadmium vapor was removed by condensation in a mass-transfer unit (MTU) consisting of countercurrent heat-exchanger trays. This unit was designed under the supervision of Erv Carls of CMT by members of the Engineering Division. In this system, a portion of the cover gas in the electrorefiner was removed, then passed through the MTU. Using the MTU, the concentration of

cadmium in the cover gas within the electrorefiner was reduced from 2,000-4,000 ppm by weight to less than 100 ppm. In the advanced IFR process flowsheet, which eliminates the cadmium pool, the concentration of cadmium vapor in the electrorefiner cover gas would be greatly reduced, possibly negating a need for the MTU.

WASTE TREATMENT PROCESSES

After an electrorefining campaign, which consists of processing about 100 kg of spent fuel, the metal and salt phases in the electrorefiner must be processed to remove accumulated fission products and to recover the TRU elements for recycle. Before salt is removed from the electrorefiner, about 90% of the actinides is removed from the salt by the uranium-plutonium drawdown procedure described previously. The reference flowsheet for treatment of the wastes is shown in Fig. 6-22.

Salt Extraction. For the salt extraction step, a high-temperature centrifugal contactor similar to that developed by ANL for aqueous/organic solutions was designed and fabricated from Type 304 stainless steel. Good performance of a single-stage contactor with a 4-cm-dia rotor was demonstrated in a glove-box facility in which the contactor was installed along with feed and receiver vessels. During countercurrent flow of the cadmium and salt, the contactor operated very smoothly—no vibration was observed and feed rates could be controlled. In tests in which cerium was used as a stand-in for uranium, lanthanum for plutonium, and yttrium for rare earths, because of the similarities in the relative separation factors, stage efficiencies of 90% were found at rotor speeds of 2,700 rpm. The results show that it should be possible to achieve good separation of the TRU elements



Plutonium and uranium are separated from the rare earth and alkaline earth elements by a countercurrent extraction process in which the uranium and TRU elements (Pu, Am, Cm) are extracted into a cadmium-2.2 wt% uranium solution. About five or six extraction stages are required to remove 99.9% of the plutonium. Essentially all the uranium, any residual TRU elements, and most of the rare earth elements are then removed from the salt raffinate by contacting it with a Cd-0.1 wt% Li alloy in a salt stripping step. The salt at this point contains all of the alkali metal, alkaline earth, and halide fission products, and only traces of actinides (<10 nCi/g). The cadmium from the salt stripping step is combined with spent metal from the electrorefiner and the cladding hulls, and the excess cadmium is removed by distillation and returned to the electrorefiner (ER). The salt and metal wastes are then converted to suitable waste forms for disposal in a high-level waste repository.

Fig. 6-22. Waste Treatment Flowsheet

from rare earths in a multistage unit. In 1995, a four-stage unit was built and installed in the glove-box facility. Flow tests showed satisfactory performance of the contactor, and the extraction tests, completed in 1997, were successful. This work was done under the direction of Terry Johnson and Lorac Chow.

Salt Stripping. Demonstrations of the salt-stripping operation were performed by use of the apparatus shown in Fig. 6-23. This apparatus was installed in an argon-filled glove box adjacent to the engineering-scale electrorefiner. Electrolyte salt from the electrorefiner was pumped into the apparatus through a heated transfer line by a submersible centrifugal pump. Because uranium had not been removed from the salt by a drawdown procedure, a cadmium-15 wt%

lithium alloy was used for reduction of the actinides, the rare earth elements, and yttrium, rather than the cadmium-0.1 wt% lithium alloy called for in the flowsheet. The experimental results shown in Fig. 6-24 agree well with predictions based on laboratory-scale experimental data. Successive additions of the reductant alloy are represented by S4 through S9 on the abscissa.

Waste Salt Immobilization. The waste salt from the salt-stripping operation will contain the fission products, cesium and strontium, and is, therefore, a high-level waste which must be disposed of in a geologic repository. Michele Lewis and others, under the supervision of Terry Johnson, investigated the use of zeolites for immobilizing the salt waste. To immobilize the salt waste, it is

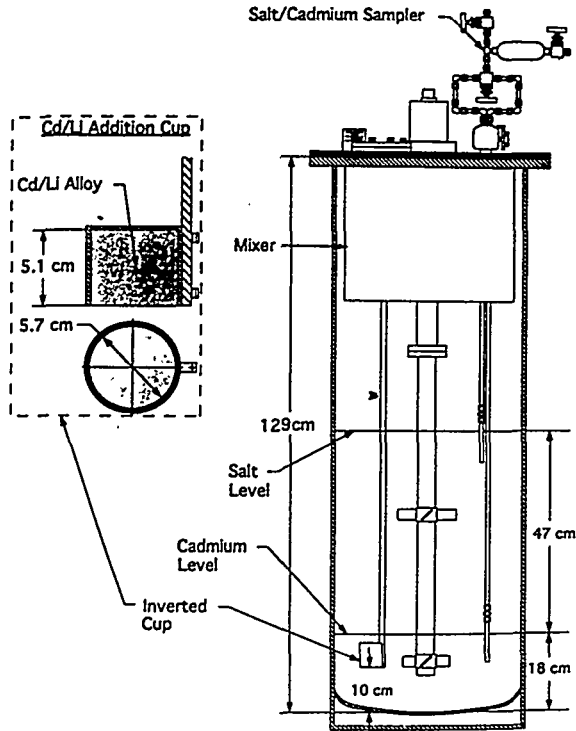


Fig. 6-23. Salt Stripping Apparatus

sorbed into a zeolite, which must then be converted to a solid waste form. The zeolite of choice is zeolite A, $M_{12}(AlO_2 \cdot SiO_2)_{12}$, where M is a cation such as sodium. Treatment of this zeolite with a pure LiCl-KCl eutectic produces $M_{24}(AlO_2 \cdot SiO_2)_{12}Cl_{12}$.

When this latter material is exposed to the IFR waste salt, the cations exchange with the fission products, removing them from the salt. Blending this material with "anhydrous" zeolite, $Na_{12}(AlO_2 \cdot SiO_2)_{12} \cdot mH_2O$, where m is 3 or 4, removes surface salt by absorption or occlusion in cages within the zeolite structure. This blended material is the starting material for preparation of the waste form. This material is stable to radiation at doses up to 10^9 rad, the maximum dose rate tested, and also to heat.

Two approaches were investigated for producing the final waste form. The first was to blend the salt-occluded zeolite powders with glass frit and to fabricate, under heat and pressure, a monolithic waste form. The second was conversion to sodalite, $Na_6(AlO_2)_6(SiO_2)_6 \cdot 2NaCl$, in which, for stoichiometric reasons, less waste salt is occluded in the zeolite. The addition of glass frit promotes conversion of the zeolite to sodalite. Under heat and pressure, a hard, monolithic waste form that is highly resistant to water leaching is produced. Accordingly, sodalite was concluded to be the superior waste form.

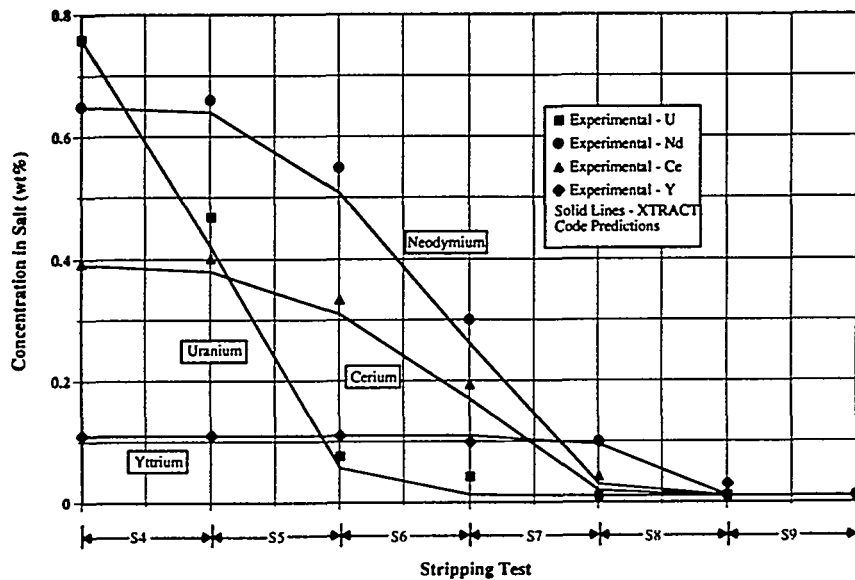


Fig. 6-24. Results of Salt Stripping Tests

Waste Metal Immobilization. The metal waste consists of cladding hulls, the cadmium-rare earth solution from the salt-stripping step, and cadmium from the electrorefiner. Removal of cadmium from this mixture for recycle by retorting was slow and difficult. The cadmium recycle load was diminished by elimination of the cadmium pool in the electrorefiner. It was found that rare earths could be extracted from the cadmium-rare earth solution into a copper-aluminum alloy, thereby allowing recycle of most of the cadmium and reducing greatly the amount going into the metal waste, but this increased the complexity of the process. Eventually, as outlined in the advanced IFR flowsheet below, the salt-stripping step was eliminated, and the rare earth elements were removed on zeolites along with the alkali and alkaline earth elements. The metal waste then consisted of cladding hulls and stainless steel filter cartridges used to remove particulate matter from the salt electrolyte. These stainless steel components containing all the noble metal fission-product elements were then simply melted together to produce a compact waste form that could easily be packaged for disposal in a geologic repository.

ADVANCED IFR FLOWSHEET

Several major flowsheet changes, listed below, were devised from work done in the early 1990s and were incorporated into an "advanced" IFR flowsheet (Fig. 6-25). They would have been demonstrated on a large scale had development of the IFR process continued.

A major feature of the advanced flowsheet is elimination of the cadmium pool to avoid problems of cadmium vaporization and condensation on surfaces of the electrorefiner. Zirconium and noble metal fission products are expected to remain largely within the anode basket. Any of them that do escape to

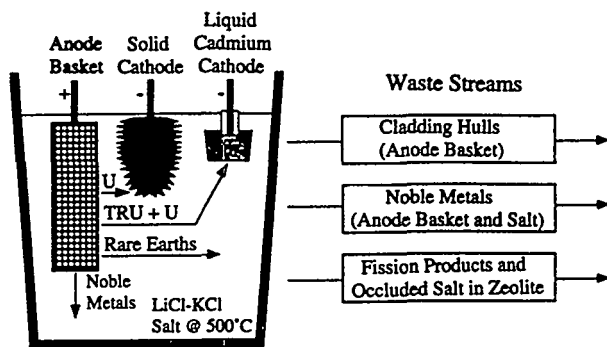


Fig. 6-25. Schematic Representation of Advanced IFR Process

the salt, where they would exist as particulates, would have to be removed by filtration.

The principal flowsheet changes are the following:

1. The volatile metals, sodium, cesium, and rubidium, would be retorted from chopped fuel pins before they are loaded into an anode basket for charging to the electrorefiner. This would permit the volatile metals to be handled separately and would prevent buildup of sodium to a point where disposal of the entire electrolyte would be required.
2. Uranium trichloride (UCl_3) rather than $CdCl_2$ would be used to oxidize chemically active fission products (alkali, alkaline earth, and rare earth metals) to their chlorides in order to maintain an actinide concentration of 2 mol% in the salt.
3. The lower cadmium pool would be eliminated from the electrorefiner. This would avoid condensation of cadmium vapor on the upper surfaces of the electrorefiner and would eliminate contamination of cladding hulls and noble metal fission product wastes by cadmium.
4. The small fraction (~10%) of the noble metal fission products that escape as particulates from the cladding hulls to

- the electrolyte salt would be removed periodically from the salt by filtration.
5. Countercurrent extraction would be used for reduction and removal of TRU elements from the salt (drawdown), for separation of the rare earth elements from the TRU elements, and for oxidation of the TRU elements back into the salt for the next electrorefining campaign.
 6. The salt-stripping step would be eliminated. The rare earth elements, as well as the alkali and alkaline earth elements, would be sorbed on zeolite for disposal. Not having to deal with a cadmium metal waste would greatly simplify the production of a metal waste form.

PERSONNEL

Jim Battles was in charge of the IFR program until he became the Division Director, whereupon Jim Laidler took over that responsibility, and he, in turn, was succeeded by Chuck McPheeters. Various portions of the program were headed up by John Ackerman, Erv Carls, Eddie Gay, Terry Johnson, and Bill Miller. Irv Johnson made major contributions to the effort by drawing on his extensive background on the chemistry and thermodynamics of liquid metal and molten salt systems. A large number of other CMT people were involved in the program: Dan Abraham, Jack Arntzen, John Basco, Bob Blaskovitz, Bob Blomquist, Lorac Chow, Jerry Dewey, Bob Everhart, Don Fischer, Greg Fletcher, Eddie Gay, John Heiberger, Len Leibowitz, Michele Lewis, Dusan Lexa, Dick Malecha, Sean McDeavitt, Chuck McPheeters, Bali Misra, Tom Mulcahey, Henry Myers, Aron Newman, Candido Pereira, Nick Quattropani, Mike Richmann, Jack Settle, Susan Slater, Mike Slawecki, Jim Smith, Ziggy Tomczuk, Verne Trevorrow, Dave Warren, and Jim Willit. A number of

Japanese scientists and engineers who participated in this effort under an international agreement made significant contributions to this research and development program. These were: Masatoshi Iizuka, Katsumasa Kanasugi, T. Kobayashi, Tadafumi Koyama, Tomohiro Nishimura, Takanari Ogata, Moriyasu Tokiwai, Yasuo Tsuchie, Takeshi Yokoo, and Takuma Yoshida. Secretaries were Lilia Barbosa and Janet Carothers.

Electrometallurgical Treatment of Spent Reactor Fuels

When development of the IFR process was terminated, work was initiated on development of electrometallurgical processes for treatment of a variety of spent nuclear fuels for disposal in a repository. The objective was a reduction of risk of chemical reactions of groundwater with fuel emplaced directly in the repository. The treatment was aimed at separating actinides, principally plutonium, and fission products and immobilizing them in waste forms that are highly resistant to attack by groundwater. Much of the technology developed for the IFR process is applicable to the electrometallurgical treatment of the spent nuclear fuels, especially electrorefining for removal of a pure uranium product. To put it simply, the difference in objectives of the IFR process and the electrometallurgical processes is that the IFR process was designed to recycle fuel to a reactor while the objective of electrometallurgical processes is the safe disposal of spent reactor fuel and other nuclear materials.

The generic electrometallurgical process consists of dismantling fuel subassemblies, chopping the fuel into segments, and charging these into an anode basket in an electrorefiner. Uranium is then transported to a solid cathode. The fission products and actinides are then placed in two stable waste forms for disposal in a repository. One is a glass-bonded sodalite into which actinides

and highly reactive fission products have been incorporated. The other is a metal waste form, principally the cladding hulls, which also contain nearly all of the noble metal fission products. There are no other high-level wastes, and only small amounts of low-level wastes are produced. Variations in this basic process had to be developed to accommodate the different types of spent fuels. In the case of reactor fuels, separation of a bulk constituent such as uranium greatly reduces the volume of waste produced for repository storage and, hence, the costs of waste disposal.

ADVANCED ELECTROREFINER CONCEPTS

To accommodate large quantities of spent fuel requiring treatment for disposal, an effort was mounted on the development of an advanced electrorefiner capable of high uranium throughput (>40 kg/h) and a batch-size capacity of 100 kg. Illustrated in Fig. 6-26 are anodic dissolution baskets in a high-throughput electrorefiner constructed in 1995 for testing. The four baskets were loaded with uranium from the lithium reduction step for converting oxide fuel from the Hanford "N" reactor to metal. The baskets are lined with

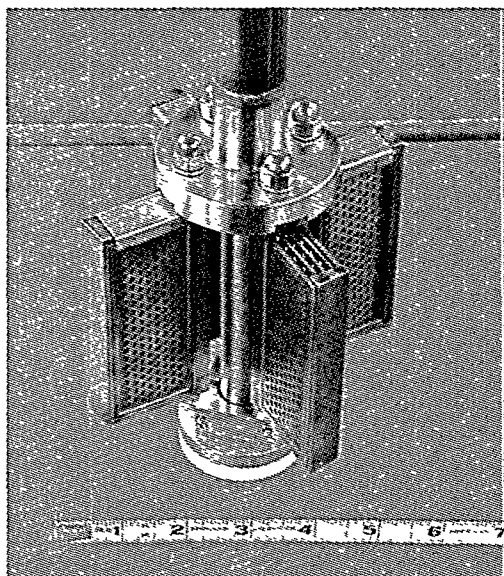


Fig. 6-26. Anodic Dissolution Baskets in Advanced Electrorefiner

325-mesh stainless steel screen to retain uranium particles from the reduction step. The cathode is a steel crucible with a salt drainage hole at the bottom. During electrorefining, the uranium is electrodeposited on the walls of the cathode crucible, scraped off the crucible by steel or beryllia scrapers attached to the ends of the rotating anodic dissolution baskets, and collected in the bottom of the crucible. After transport of the uranium has been completed, the anodic dissolution baskets are replaced by a compactor to compact the uranium to a density greater than 10 g/cm^3 . The uranium is removed and melted to produce a uranium product ingot.

Short circuits plagued the initial runs using U-Zr-fissium pin segments (EBR-II-type fuel) as a result of which the number of ampere-hours required to transport a kilogram of uranium was very high. Uranium transport rates were very low—only about 60 g of uranium per hour. Design improvements were needed to achieve high uranium throughput.

Effort continued on a high-throughput electrorefiner (HTER) design with a uranium throughput capacity of >40 kg U/h and a batch size of 100 kg. The HTER consists of 20 stainless steel anode baskets and has a batch size of 150 kg. This electrorefiner, with a diameter of 25 in. (0.6 m), accommodated a uranium batch size of 150 kg in tests conducted with unirradiated "N" reactor fuel. The number of ampere-hours (31,219) was nearly twice the number of ampere-hours passed through the electrorefiner in all the earlier runs. About 75 kg of uranium was collected from the tests, and about 50 kg of that uranium was transferred to a cathode processor for consolidation. The limiting factor in the scaleup was the scraper arrangement for removing the uranium product from the cathode tubes. These initial scaleup tests were considered successful, and more favorable operating conditions along with improved scraper blade designs are expected to extend the operating time of the unit.

PROCESS DEVELOPMENT STUDIES

Process flowsheets are being developed for the following types of reactor fuels.

Spent Fuel from Experimental Breeder Reactor-II. When plutonium disposal, rather than recovery, is the objective, the treatment process becomes much simpler than the IFR process, which was designed for recovery and recycle of plutonium from the U-Pu-Zr fuel alloy. In particular, the salt-extraction and salt-stripping steps can be eliminated. Following a campaign in which uranium is removed from ten batches of fuel (about 100 kg) by electrotransport to a solid cathode mandrel, the actinides can be removed from the salt (drawdown) by the lithium-ion displacement procedure described previously under the IFR pyrochemical process. (An alternative to drawdown by electrotransport, which is gaining favor, is a chemical extraction of uranium and plutonium into cadmium by a countercurrent extractor.) The uranium and plutonium concentrations in the salt electrolyte would be restored by converting them to the chlorides with CdCl_2 . The alkali, alkaline earth, and rare earth fission products can then be sorbed on a zeolite, which is converted to a waste form for disposal. Alternatively, uranium alone can be removed from the electrolyte, and plutonium, together with the highly reactive fission products, can be sorbed on the zeolite. Experimental results showed that the amount of plutonium sorbed on Zeolite A was substantial—up to 22 wt%. Thus, Zeolite A appears to be a good candidate for removing plutonium from waste electrolyte salt.

The dendritic uranium deposit resulting from the electrotransport of uranium is wetted by the electrolyte salt, which contains plutonium and fission products. To produce a pure uranium product that does not have to be sent to a geologic repository, it is necessary to remove the contaminated salt. It was found

that washing with a salt that is in contact with lithium dissolved in a molten metal such as cadmium is effective. Two successive washings resulted in complete removal of the rare earth elements. The final rare earth concentrations in the washed salt containing the uranium were generally below the limits of analytical detection (<0.01 wt%). Plutonium was not present in these experiments, but its behavior should be the same as that of the rare earths.

The metal waste consists of (1) the cladding hulls along with most of the noble metal fission products (about 92% according to experimental results) and (2) filter cartridges, which remove residual noble metals and uranium oxide from the molten salt. The metal waste would be melted to form an ingot.

The "Mark V" high-throughput electrorefiner, with a diameter of 10 in. (0.2 m) and a capacity of 150 kg/month, is being readied for a demonstration of EBR-II blanket processing at ANL-West.

"N" Reactor Fuel. Located at Hanford, the "N" reactor uses a uranium oxide fuel clad with Zircaloy. After reduction with lithium to convert the uranium oxide to the metal, which is discussed later, the reduced metal is made the anode of an electrorefiner and electrotransported to a solid cathode. Treatment for disposal of the fission products can be effected with only slight modifications of the process described above for EBR-II fuel.

Single-Pass Reactor Fuel. Single-pass reactor (SPR) fuel consists of aluminum-clad uranium slugs bonded by an Al-Si braze. Opening up the cladding to permit removal of the uranium by electrotransport was accomplished by drawing a cutting blade longitudinally along the surface of the SPR fuel element and laying open the cladding. With a simulated SPR fuel element used as an anode in a test cell, the uranium was successfully

transported to a solid cathode. The mass of the aluminum sheath remained constant, and there was no evidence of corrosion. This work demonstrated that uranium can be selectively oxidized in the presence of aluminum at a reasonable current density and a current efficiency of 75%.

Aluminum-Based Spent Fuels. Over the next forty years, 128 metric tons of spent aluminum-matrix reactor fuel will be shipped to the Savannah River Site from U.S. and foreign research reactors. When fabricated initially, this fuel contained over 55 metric tons of uranium at an average enrichment of approximately 20% U-235. This fuel is now corroding in wet storage and must be stabilized. The fuel would normally be processed in the Savannah River processing facilities, but these are slated for decommissioning in 2005.

Electrometallurgical treatment was regarded favorably by a special DOE task team formed to look into the treatment, packaging, and disposal of these fuels because the method has the potential to separate aluminum and uranium, thus greatly reducing the amount of high-level waste with an estimated cost saving of \$200 million. The enriched uranium has a commercial value of about \$400 million.

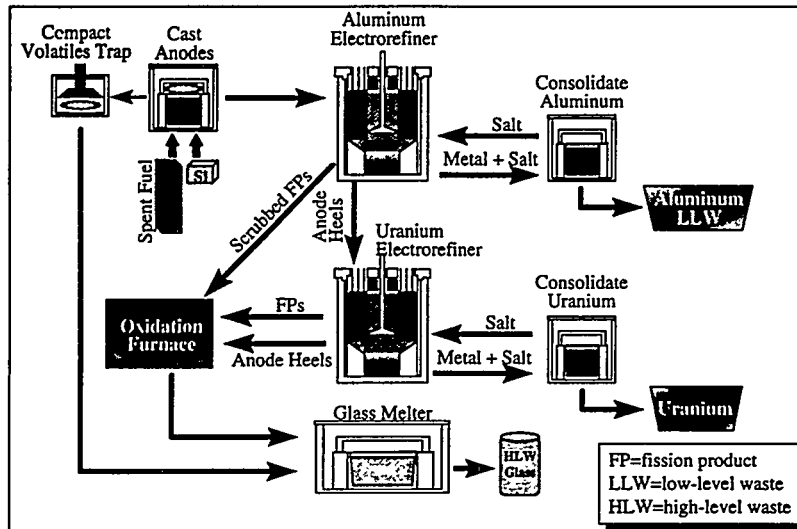
The proposed flowsheet for aluminum-based fuels is shown in Fig. 6-27.

Waste Salt from the Molten Salt Reactor Experiment (MSRE). The Molten Salt Reactor, which was operated at Oak Ridge in the 1960s, used a uranium fluoride fuel that was dissolved in a mixture of fluoride salts. Initially, ^{235}U was the fissionable material, but this was changed later to ^{233}U . The fuel salt has been in storage at ORNL since 1969 when the reactor was shut down. A small amount of ^{232}U , which has a half-life of 70 years, was produced during reactor irradiation. In its decay chain is thallium-208, which emits hard

(2.6-MeV) gamma radiation. Irradiation of the fluoride salts by this gamma and that resulting from fission-product decay cause decomposition of the fluoride salts with the production of fluorine gas (F_2). Some of the fluorine reacts with UF_3 to form UF_6 , whose high volatility leads to migration of uranium and the spread of activity throughout the storage system. Cleanup of the salt by removal of the fission products and recovery of the ^{233}U has become a matter of high priority.

One of the methods under consideration for salt cleanup is an electrometallurgical process proposed by the CMT Division. In this process, a lithium-bismuth alloy is used as the anode in an electrochemical cell, and constituents of the salt are successively reduced in four steps by lithium-ion displacement. In the first step, noble metal fission products and most of the zirconium are deposited onto a solid cathode. In the second step, uranium, TRU elements, and the rest of the zirconium are deposited on a solid cathode. The bismuth of this step is made the anode of a second electrorefiner to purify and isolate U-233. In the third and fourth steps, rare earths, alkaline earths, thorium, cesium, and barium are also removed to liquid bismuth cathodes by using increasingly higher voltages. This leaves the salt essentially devoid of activity and disposable as a low-level waste. Construction was begun in 1995 on an electrorefining cell suitable for work with fluorides at temperatures up to 700°C.

The remediation process proposed by ANL for the MSRE salt is to separate the salt into actinides for recovery, fission products for disposal as high-level waste, and bulk salt for disposal as low-level waste. The total salt volume of about 2000 L would be processed in 30-L batches in a lightly shielded facility. Seventeen tests were made. A solid cathode and simulated MSRE salt were employed to investigate the removal of zirconium and its separation from uranium. Lithium-bismuth alloy was used in the anode baskets. The



Following removal of the end hardware, the fuel is melted and cast into shapes for use as anodes in the succeeding electrorefining operations. Silicon is added to form stable intermetallic compounds with the uranium and enhance the separation of aluminum in the first electrorefining step. A cryolite electrolyte (Na_3AlF_6) is used for the electrotransport of aluminum. The anode basket is then transferred to a uranium electrorefiner in which the electrolyte is the LiCl-KCl eutectic, and uranium is transported to a solid cathode. High rates for the product metals are achieved by use of the high-throughput advanced electrorefiner described earlier. The product metal dendrites are consolidated by melting. The lower melting electrolytes that adhere to the dendrites are poured off and recycled after the product metals have solidified. Fission products from various sources are converted into oxides, combined with glass formers, and melted to produce a glass waste form, which is placed in a canister for emplacement in a geologic repository.

Fig. 6-27. Flowsheet for Electrometallurgical Treatment of Aluminum-Based Fuel

results indicated that zirconium (along with other noble metals in the salt) can be separated from the salt by deposition on an iron cathode. This material could be converted into a stable metal waste form. Any remaining zirconium and all the uranium can then be deposited on a second solid cathode. The process concept shows promise, but further work is needed on the details, one of which is removal of cesium from the salt.

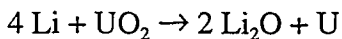
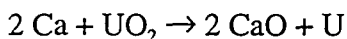
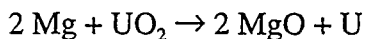
ACTINIDE RECOVERY FROM SPENT OXIDE FUELS

Spent fuel from commercial, water-cooled power reactors (LWRs) contains significant amounts of unreacted fissile uranium as well as TRU elements (Np, Pu, Am, and Cm). Separation and recovery of these elements from the spent fuel would offer two major benefits: (1) these actinide elements could be

a useful source of additional energy if burned in a fast reactor and (2) removal of these elements, which have long half-lives, from the spent fuel would considerably shorten the time required for assured confinement in a geologic repository. In the early 1990s, this was a natural companion program with the pyrochemical process for IFR fuel.

Because of a national policy decision to discontinue all work on fast reactors in 1993, actinide recycle became a dead issue, and these programs were phased out. It was realized, however, that the capabilities of such processes could be redirected toward much-needed methods for treating various types of oxide fuels for safe disposal. Adaptation of the lithium reduction process (to be described later) for this purpose is the subject of the next section on "Treatment of Spent Oxide Fuels for Safe Disposal."

The work on this process drew heavily from previous technology that had been developed during the development of processes for EBR-II fuel and subsequent work. Four processing schemes were investigated, all of which involved a reduction of the UO_2 fuel to uranium metal, followed by separation steps to recover the uranium and TRU elements. Three reactive metals—magnesium, calcium, and lithium—were evaluated as candidate reductants for the UO_2 . All three are capable of reducing the UO_2 in molten salt solutions, but each one presents its own set of problems. The reduction reactions are



To avoid the production of large amounts of radioactive MgO , CaO , or Li_2O by-product waste, an electrowinning step is considered necessary to regenerate the Mg, Ca, or Li for

recycle. Electrowinning of these metals from the oxides is a difficult operation and has been avoided by industry, but initial studies indicated that it might be feasible for this purpose. Direct electrolytic reduction of UO_2 to the metal has also been tried with limited success. In all cases, the main problem appears to be the lack of a satisfactory anode for oxygen release. Although earlier work had shown that magnesium-zinc alloys could be used to reduce UO_2 , only calcium and lithium were used as reductants in the actinide recycle program.

After the UO_2 reduction, several approaches are available for separation of the uranium, TRU elements, fission products, and other fuel constituents. Among these are salt transport, magnesium extraction, precipitation in zinc-magnesium, halide slagging, and electrorefining.

Salt Transport Process. In this process, the oxide fuel was first reduced by calcium in a $\text{Mg-Cu/CaCl}_2\text{-CaF}_2$ system to produce a Cu-Mg alloy containing the TRU elements and some fission products. The reduced uranium precipitated because of its low solubility in the alloy. Alkali, alkaline earth, and halide fission products remained in the salt, and the gaseous fission products were released. In the ensuing salt transport step, the Cu-Mg alloy and a Zn-Mg alloy in mutual contact with a molten salt were equilibrated, causing the actinide elements to transfer to the Zn-Mg alloy. The more noble metals and the uranium remained in the Cu-Mg alloy. The TRU elements and rare earths were recovered by evaporating the Zn and Mg and were transferred to the IFR electrorefiner, where they were introduced into the IFR fuel. The CaO from the UO_2 reduction was electrolyzed to produce metallic calcium for recycle.

In initial tests using UO_2 , PuO_2 , NpO_2 , and oxides of representative fission-product elements, the reduction step was effective, and the salt transport separation was as

expected. However, significant coprecipitation of neptunium with the uranium necessitated the addition of a halide slagging step to recover the neptunium from the uranium when it was melted to form a U-Fe product ingot.

Investigations of this process were discontinued in favor of the lithium reduction process in 1992. However, the significant body of information on the thermodynamic, chemical, and electrochemical processes involved in the salt-transport process and on materials compatibility that had been developed during the work by Irv Johnson and others on this process became a highly useful database for the ongoing development programs in this area.

Magnesium Extraction Process. The head-end steps of the magnesium extraction process were essentially the same as those for the salt-transport process; that is, the UO_2 fuel was reduced by calcium in a $\text{CaCl}_2\text{-CaF}_2$ molten salt at about 800°C . To obtain a liquid phase, the reduced uranium was alloyed with iron. The U-Fe alloy was then contacted with liquid magnesium, which extracted the TRU elements and some of the rare earth metals, leaving behind the U-Fe, noble metals, and the rest of the rare earths. The magnesium was removed from the TRU elements by retorting, and the TRU product was used as a feed to the IFR fuel cycle.

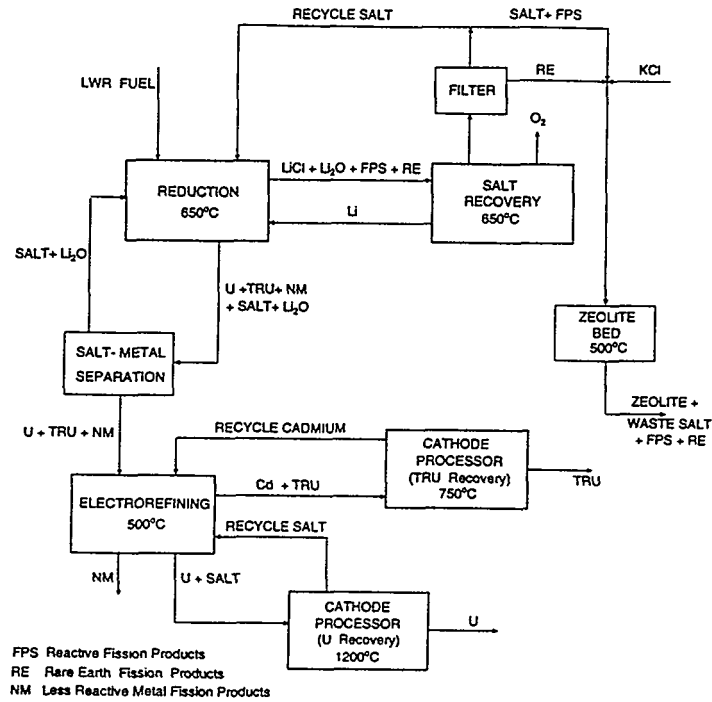
Two runs were made at 790°C with synthetic LWR fuel containing UO_2 , PuO_2 , and NpO_2 , along with oxides of fission product elements, to evaluate the process. The reductions were satisfactory, but the extraction results were somewhat inconclusive, due mainly to poor material balances. Further work showed that multiple extractions would be required, and, as in the salt-transport process, a halide slagging step would be needed to recover neptunium from the uranium. Because of these problems and

difficulties with materials compatibility, work on this process was discontinued in 1991.

Zinc-Magnesium Process. Again, the UO_2 fuel was reduced by calcium in $\text{CaCl}_2\text{-CaF}_2$, but in this case the TRU elements and uranium metal were collected in a magnesium-rich Mg-Zn alloy in which the uranium has a low solubility and precipitates as the metal. The Mg-Zn alloy containing the TRU elements was separated from the precipitated uranium and then retorted to vaporize the zinc and magnesium, leaving an ingot of the TRU elements to be added to the IFR electrorefiner. The uranium precipitate was cast into an ingot for storage. Because about 20% of the neptunium coprecipitated with the uranium in the process, a $\text{CaCl}_2\text{-UCl}_3$ salt was used in the uranium casting step to extract the neptunium into the salt phase, which was recycled to the reduction step to complete the neptunium recovery. Work on this process was terminated in 1992.

Lithium Reduction Process. In 1992, work began on another alternative process which employs lithium as the UO_2 reductant. A flowsheet for the lithium reduction process is shown in Fig. 6-28. In 1992, the lithium reduction process was selected for continuing development work on actinide recycle. As mentioned earlier, however, the program was redirected to the treatment of oxide fuels for disposal, rather than recovery of the actinides.

Laboratory-scale (0.5-kg) experiments showed that 99.99% reduction of the actinide oxides could be achieved. The reduction, uranium electrotransport, and uranium consolidation steps were performed by using simulated oxide fuel containing oxides of uranium, plutonium, neptunium, curium, and fission products. Reasonable material balances were obtained, and the basic feasibility of the process was established. Engineering-scale equipment capable of



The oxide fuel is reduced with lithium in the presence of molten LiCl-KCl at 500°C (later changed to LiCl alone at 650°C). The spent reduction salt is then processed electrochemically to decompose the Li₂O reduction product and recover lithium and LiCl-KCl. A small portion of the recovered salt is removed to limit the accumulation of unreduced fission products (*e.g.*, Cs, Sr, I, and rare earths), and the bulk of the salt and the recovered lithium are recycled. The removed salt is processed for disposal by methods outlined under the IFR process. After separation from the reduction salt, reduced fuel and less reactive fission products (*e.g.*, Zr, Mo, and Pd), which precipitate during the reduction step, are processed in an electrorefiner to recover purified uranium on a solid cathode. The TRU elements are recovered in a liquid cadmium cathode. The uranium is stripped from the cathode, melted, and recovered as an ingot. The TRU product is recovered as an ingot by distilling off the cadmium for recycle. The uranium is placed in long-term storage for future use as a reactor blanket material, and the TRU ingot is fed into the IFR fuel cycle.

Fig. 6-28. Lithium Process Flowsheet

handling up to 20-kg batches of simulated fuel was designed, fabricated, and installed in controlled-atmosphere glove boxes.

TREATMENT OF SPENT OXIDE FUELS FOR SAFE DISPOSAL

In the electrometallurgical processing of spent reactor fuels, oxide fuels consisting primarily of uranium dioxide (UO_2) present a problem because the oxides must first be reduced to the metals before the fuel can be processed in an electrorefiner. Lithium metal, an exceptionally strong reducing agent, was selected for this purpose to assure as rapid and complete reduction as possible. Molten lithium chloride (LiCl) at a temperature of about 650°C was chosen for the process medium. To avoid the production of wastes containing large quantities of Li_2O produced by this reaction, a lithium electrowinning step is incorporated into the process flowsheet:



By recycle of the lithium, the net effect is an electrolytic reduction of UO_2 to produce uranium metal and oxygen. In theory, direct electrowinning of uranium from UO_2 is possible, but previous attempts to do so had shown that it was difficult, so the use of lithium as an intermediate reductant was adopted for the process development effort. It is possible, however, to carry out the two reactions simultaneously in a single process vessel. Subsequent electrorefining purifies the uranium metal product, which can then either be enriched for recycle or be converted to a form suitable for storage or disposal as a low-level waste. In the electrorefining step, the TRU elements (Np, Pu, Am, Cm) can be recovered and alloyed with cladding material and combined with fission products to produce a leach-resistant and diversion-resistant form for ultimate disposal. An

alternative is to combine the TRU elements and fission products in a ceramic waste form.

Processing of the TMI-2 Core Debris. The emphasis in this program was largely on a process for the treatment of the debris resulting from the accident at the Three Mile Island-2 reactor in March 1979. This would be a stringent test of the process capabilities in view of the fact that the debris is a highly heterogeneous mixture of oxides, mainly of uranium and zirconium, and a variety of metals from the fuel cladding and other reactor hardware. The debris was divided into four parts, depending on the location in the core and the degree of damage at that location: (1) essentially undamaged fuel near the bottom of the reactor, (2) a portion in the center of the core, which had melted, producing a mixture mainly of $(\text{U,Zr})\text{O}_2$ ceramic phases, (3) an upper crust region, surrounding the part of the core that had melted and consisting of the ceramic phases and metallic components that had melted, and (4) a similar lower crust region. If a process can be developed to handle this material, it should be able to cope with almost any UO_2 -based system.

Four process flowsheets were developed for treating the TMI-2 debris. The first was similar to one developed earlier for processing normal spent fuel from a light water reactor. The second flowsheet was designed to accommodate the mixed ceramic melt $(\text{U,Zr})\text{O}_2$, which contained uranium- and zirconium-rich phases. The third and fourth flowsheets were intended to handle agglomerates of metallic and ceramic phases of widely different ceramic/metal ratios. A suitable substitute for TMI-2 core debris that could be used for some laboratory- and engineering-scale experiments was available from other ANL reactor safety programs in the form of "corium," which is a synthetic molten core material consisting (in wt%) of

58 UO₂, 11 ZrO₂, 14 Zr, 14 Fe, and 3 Cr. This material was used to test the process flowsheets.

Anode Materials and Designs. In the lithium electrowinning operation, the oxygen produced at the anode in the molten LiCl is an aggressive oxidizing agent. This condition severely limits the choice of materials for the anode, which must be both resistant to oxidation and electronically conductive. Carbon, or graphite, which is sometimes used as an anode in corrosive environments as a sacrificial electrode (producing CO or CO₂, rather than oxygen), is unsatisfactory because the molten salt becomes contaminated by carbon particles. Platinum or a platinum-rhodium alloy was used in most of the experimental work, but it is attacked by metallic lithium. An effort is underway to develop an electronically conductive oxide ceramic (similar to those used in fuel cells) or other alternative materials. Possible oxide ceramics include Fe₃O₄, antimony-doped tin oxide, and lithium-doped nickel oxide.

During the electrowinning of lithium from Li₂O in the LiCl salt, gaseous oxygen is generated at the anode. Ideally, the oxygen would be removed from the system immediately by forming bubbles that escape from the molten salt. What actually happened was that the oxygen generated at the anode surface formed very small bubbles that were slow to coalesce and disengage. Although a shroud had been installed around the anode to confine the oxygen, the very small oxygen bubbles appeared to form a quasi-homogeneous lighter phase with the salt, which created a stagnant region within the shroud, thereby forcing new bubbles into the bulk salt as they were formed. This oxygen was then transported by the salt flow to the cathode where it recombined with the metallic lithium. Design studies of this system resulted in a modified anode design that was used in engineering-scale studies (see Fig. 6-29).

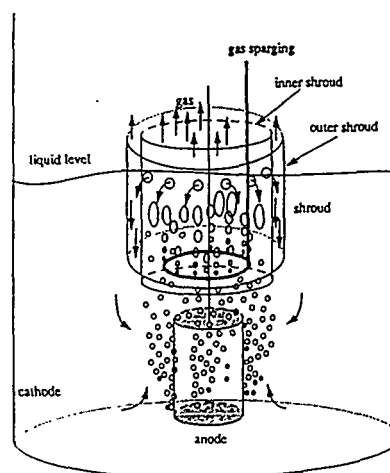


Fig. 6-29. Anode Design for Electrowinning Lithium from Lithium Oxide

Cathode Materials and Designs. Two types of cathodes, liquid bismuth and porous metal, were investigated with the objective of decreasing or eliminating the recombination of oxygen in the electrolyte with the lithium metal product. When lithium is electro-deposited into liquid bismuth, its chemical activity is decreased markedly (by a factor of 10^3 to 10^6) due to the formation of intermetallic compounds. The densities of the bismuth and the intermetallic compounds are much higher than that of the electrolyte salt. The limited surface area of the bismuth electrode and the low activity of the lithium tend to protect the lithium from the oxygen in the electrolyte. The confinement of lithium in the bismuth and its low activity also tend to protect platinum anodes from lithium attack. The bismuth cathode, however, requires an additional process step to recover the lithium and a suitable ceramic containment material.

Porous metals are available in a variety of materials and forms, including screens, felts, and foams. Other work had shown that porous stainless steel was readily wet by liquid lithium and that repeated electrolytic

deposition and removal of lithium from porous stainless steel electrodes was a viable process operation. The lithium remains within the electrode in the molten salt medium, so there is no need for crucibles or other ceramic parts.

Uranium Dioxide Reduction. In 1995, two preliminary experiments were performed to determine whether the chemical uranium reduction and the lithium electrowinning steps could be combined into a single operation that would be, in effect, a direct electrolytic reduction of the UO_2 . A sketch of the cell that was used is shown in Fig. 6-30. The anode was a Pt-Rh tube, housed in a MgO shroud that was open at the bottom. The cathode was a cylindrical basket made of stainless steel screen. The cathode was connected to a stainless steel tube that served both as the electrical lead and as a helium-gas purge tube for the cell to minimize the oxygen concentration in the gas phase during the electrolysis. The cell container was a high-density MgO crucible. The two reduction experiments were similar, except 100 g of UO_2 chips was used in the first one and only 55 g was used in the second. The cell was operated at a temperature of 650°C , a constant potential of 3.0 V, and a time period of about 30 h. In the first experiment, in which about

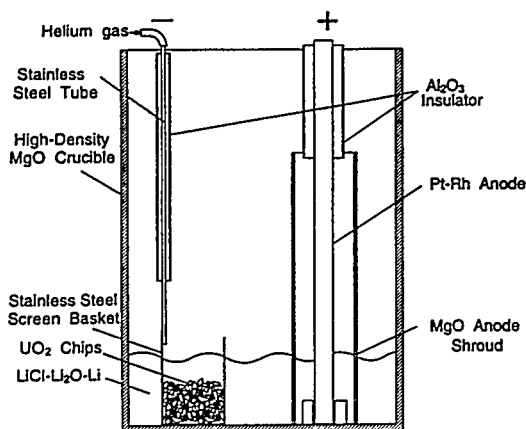


Fig. 6-30. Experimental Cell for Uranium Oxide Reduction

105% of the theoretical current was passed, some of the interiors of the UO_2 chips still contained unreacted UO_2 . In the second experiment, in which 140% of the theoretical current was passed, the reduction to uranium metal was complete. Thus, the direct electrolytic reduction of UO_2 was shown to be possible.

The reduction studies, using steel-clad UO_2 pellets as the feed, were continued. The pellets, which were 1.27-cm long and 0.95-cm dia, were completely reduced in approximately 50 h; unclad pellets of the same size required 30 h. During the reduction, the pellets retained their original size and shape, and voids were created due to the fact that the uranium product has a higher density than the UO_2 . The voids were filled with the LiCl electrolyte salt, which contained dissolved Li_2O . In a process, the Li_2O concentration would have to be kept below 3.3 wt% to achieve complete reduction of any PuO_2 that may be present. In the case of TMI-2 fuel debris, Li_2ZrO_3 can be formed unless the Li_2O concentration in the salt is held below 1.4 wt%. Although the direct electrolytic reduction of UO_2 had been demonstrated in the earlier experiments, it was clear that development work would be required to achieve higher reduction rates and to manage the Li_2O concentration in the electrolyte. Among the specific problems to be addressed are physical pretreatments of the feed material such as crushing or grinding, the design of the process cell, and suitable materials of construction. None of these problems appears to be "show-stoppers," but a significant effort may be required to solve them.

Fission-Product Behavior. At the anode of the electrolysis cell, tellurium, which is a fission product, tended to form an insulating layer of compounds on the Pt-Rh electrode. Removal of the tellurium by a sacrificial molybdenum electrode prior to the lithium electrowinning step proved to be effective.

The behavior of rare earth fission products was complicated by the fact that the rare earths did not all behave similarly. The sesquioxides (RE_2O_3) were converted to the mixed oxides (LiREO_2) under certain conditions, and the rare earths had a strong mutual influence on one another in the molten salt solution. Studies were conducted in which rare earth oxides were equilibrated with molten LiCl that was saturated with lithium and contained varying concentrations of Li_2O at 650°C . The concentrations of Nd and Ce increased, and those of Eu and Sm decreased with increasing Li_2O concentration. When the LiCl salt did not contain elemental lithium, the concentrations of Eu and Sm were decreased significantly. Mixed oxides, LiREO_2 , formed in all cases when the Li_2O concentration reached a high enough level. Free energies of formation of LiREO_2 compounds were calculated from the transition points (Li_2O concentrations) for the change from sesquioxides to mixed oxides.

Engineering-Scale Demonstration. The engineering-scale facilities consist of a large ($7.6 \times 2.4 \times 2.6$ m) glove box with an argon atmosphere, and a smaller one ($2.4 \times 1.1 \times$

2.6 m) with a nitrogen atmosphere. The two boxes are connected by a transfer lock. The equipment is designed to demonstrate the reduction, electrowinning, casting, oxidation, drying, and retorting steps of the process. A cutaway view of the equipment is shown in Fig. 6-31.

An initial reduction run using the lithium process and LiCl-KCl salt at 500°C was made in 1993 with 4.4 kg of UO_2 -based simulated fuel. The product was a very fine metal precipitate that could not be melted into ingots or recovered by electrorefining. New process equipment was installed in the argon glove box in 1994, and two experiments were run in 1995. The first runs, conducted at 650°C with LiCl salt and 10 kg of UO_2 simulated fuel, were successful in reducing the uranium, but not in regenerating the spent salt by the lithium electrowinning step. Engineering-scale reductions of synthetic corium (mainly UO_2 and ZrO_2) and simulated TMI-2 fuel were conducted in 1996. Neither reduction was complete, apparently due to an underestimation of the required time based on the laboratory data.

Development work was then continued both on the reduction and the electrowinning

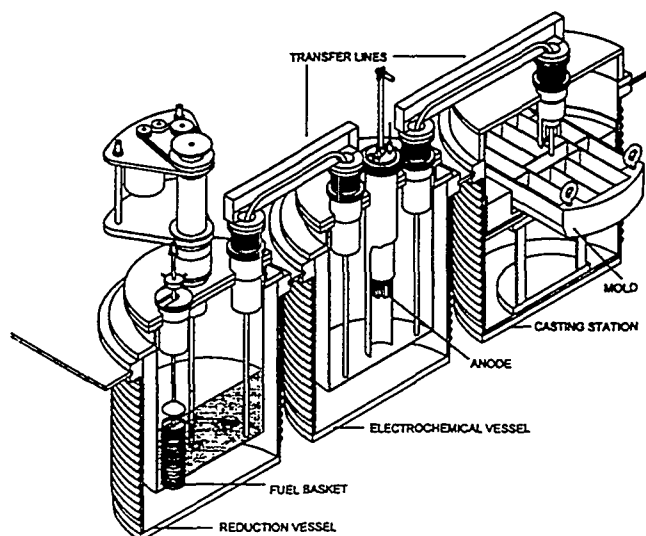


Fig. 6-31. Engineering-Scale Electrometallurgical Processing Facility

steps of the lithium reduction process, as well as scaleup and materials studies. In the electrowinning step, recombination of the oxygen and metallic lithium products was identified as a problem, which was solved by electrodepositing the lithium in a porous metal cathode. The lithium wets the porous metal (stainless steel) and is retained in the pores. Another major problem with the electrowinning step is the cost of the Pt-Rh anodes that were being used. A study was initiated on the possibility of replacing the Pt-Rh alloy with electronically conductive ceramics such as Fe_3O_4 , SnO_2 , or NiO . Other continuing experiments showed that complete reductions of about 3-4 kg of UO_2 could be achieved in the engineering-scale equipment, but that design improvements were needed to increase the reduction rates.

Treatment of INEEL Spent Fuel. The inventory of spent fuel at the Idaho National Engineering and Environmental Laboratory contains a variety of fuel types that are unsuitable for direct disposal. Examples of these are metallic fuels, ceramic-matrix oxides, hydride and carbide fuels, and components of metallic fuels that may have reacted with water while in storage. Studies are being made to determine whether the electrometallurgical treatment could convert these materials into a uniform set of three waste streams (metallic uranium, a metal waste form, and a ceramic waste form).

PERSONNEL

This program, under Chuck McPheeters's part of the Division, was directed by Dean Pierce, until his retirement, when Jerry Johnson assumed the responsibility. Jerry, unfortunately, died of cancer in 1997, and Eric Karell took his place. Other members of the group included Bob Everhart, Karthick Gourishankar, Tom Mulcahey, Dave Poa, Jim

Smith, Mike Vest, Dave Warren, and Eugene Wesolowski.

Fusion-Related Research

Work continued on fusion-reactor research, with emphasis on the feasibility of using lithium-containing oxide ceramics as the blanket fuel. Safety and cost considerations make it desirable to minimize the inventory of tritium in a fusion reactor system, but sufficient amounts must be available to start up the reactor and operate it in a self-sufficient manner. These conflicting requirements are complex and require modeling, which, in turn, depends upon reliable experimental information. Most of the CMT work in the 1990s was oriented toward tritium generation, recovery, and handling in the breeder blanket and associated equipment.

DESORPTION MEASUREMENTS FOR $\text{LiAlO}_2\text{-H}_2\text{-H}_2\text{O(g)}$ SYSTEM

Temperature-programmed desorption (TPD) was used to measure activation energies and other kinetic factors relating to desorption of H_2O and H_2 from LiAlO_2 in helium and helium-hydrogen streams. The hydrogen was expected to promote tritium release in a helium purge gas. In TPD tests, which were conducted at temperatures up to about 600°C , H_2O was evolved, both in pure helium and in helium containing up to 990 ppm H_2 . Three peaks in plots of the H_2O evolution were attributed to different sites on the LiAlO_2 . Activation energies were ~18, 23, and 28 kcal/mol, respectively, for the three sites. The first-order kinetics of the reactions were not consistent with the conventional wisdom that desorption was a bimolecular process involving the recombination of chemisorbed OH^- ions. An alternative possibility is that the process consists of bimolecular combination of OH^- and H_2O on the surface, followed by unimolecular desorption of H_2O . In a

continuation of this study, additional experimental results indicated that the rates and amounts of H₂O desorption were substantially higher with He-H₂ mixtures than with helium alone.

TRITIUM RELEASE STUDIES

Because there was some conflict between the CMT results on the desorption mechanism and those from other work, the validity of the CMT model was tested by comparing its predictions with tritium release data from in-pile and laboratory experiments.

In-Pile Experiments. In a reactor experiment, the effects of neutron flux, and therefore the tritium generation rates, on tritium release from Li₄SiO₄ and Li₂ZrO₃ samples, were determined. The tritium residence times (inventory/generation rate) were independent of flux, and the rate-controlling mechanism was not second order in tritium. Other factors indicated that desorption was the rate-controlling step for these samples, and desorption was first order under these conditions. In other tests, the tritium inventory was found to increase with increasing grain size of the samples. An analysis of the data showed that the rate of tritium release into a He-1% H₂ purge gas was not controlled by diffusion processes. Other tests employing purge gases consisting of helium with 1.0% H₂, 0.1% H₂, or 50 ppm H₂ + 100 ppm H₂O indicated that tritium release was better for the gas containing 1.0% H₂ than the one with 0.1% H₂, but the activation energies were the same. The activation energy for the He-H₂-H₂O mixture, however, was lower. These studies suggest that the activation energy for tritium desorption depends on the hydroxide surface concentration.

The SIBELIUS experiment was a joint CMT/European effort to identify performance-limiting factors connected with the use of beryllium neutron multipliers in

ceramic breeder blankets. These reflector materials generally remain in place for years at low temperatures (<100°C), and when they are annealed they tend to release the tritium as bursts at high temperatures. Experiments were conducted in the Siloe reactor at Grenoble, France, in which the behavior of beryllium disks located adjacent to stainless steel was compared with that of disks adjacent to ceramic blanket material. Because of the many variables involved, the results were not unequivocal, but it appeared that a lower density beryllium and operating temperatures above about 500°C would be desirable. In a continuation of these studies in 1994, tests were made on the compatibility of Li₂ZrO₃, Li₂O, Li₄SiO₄, and LiAlO₂ with beryllium components when they were in close contact in a neutron environment. No detrimental effects were observed on the performance of the ceramics, and chemical interactions of the two materials were negligible. It was concluded that the tritium inventories for all the ceramics should not cause any safety problems.

Laboratory Experiments. In a joint study with Commissariat à l'Énergie Atomique, Centre de Saclay, France, tritium release experiments were conducted on sintered LiAlO₂ pellets similar to those used in the in-pile studies. The kinetics and rate constants of the release behavior were essentially identical to those observed in the in-pile experiments. One difference, however, was that tritium was retained in the solid at low temperatures, even after extended annealing times at 538°C, and was released only when heated to 850°C. The retained tritium suggests that it may exist in two different forms in the solid material.

The TPD method was used to investigate tritium release from single crystals of LiAlO₂, Mg-doped LiAlO₂, and Pt-coated LiAlO₂. The TPD plot for LiAlO₂ showed five different peaks, each with a different activation energy. The magnesium doping and the platinum

coating both shifted the peaks to lower activation energies. This finding suggested that the rate-controlling step involved the surface and not bulk diffusion. These TPD results provided a basis for the development of a tritium release model that, unlike earlier models, required no adjustable input parameters. Calculated results from the model showed excellent agreement with measurements from an in-pile tritium release experiment with LiAlO_2 .

Further studies were made to obtain diffusivity and desorption rate constants for Mg-doped and undoped samples of LiAlO_2 at temperatures of 528-785°C. The results showed that tritium transport was controlled by desorption when the grain radii in the sample were less than 100 μm . Lithium titanate (Li_2TiO_2) is an alternative low-activation ceramic that was of interest as a candidate blanket material for fusion reactors, but very little tritium-release work had been done on it. Several tritium-release tests were conducted to extend the database on Li_2TiO_2 . General conclusions from the results were as follows:

1. Tritium was released at temperatures as low as 300°C, which compares favorably with the behavior of other ceramic blanket materials.
2. Several different types of sites in the crystals were involved in the release.
3. Addition of hydrogen to the helium purge gas was detrimental to tritium recovery; this was not the case for the other ceramic breeder materials.

More detailed studies of tritium desorption from Li_2O were made by a combination of TPD and diffuse reflectance infrared Fourier transform spectroscopy (DRIFTS). These experiments were performed with a purge gas of argon containing 0.1% hydrogen (or deuterium) at temperatures between 100 and 400°C. The results indicated that the

desorption was a relatively complicated process that involved different reaction sites, adsorbed species, and activation energies. In addition to the experimental work, theoretical studies of the desorption mechanism were undertaken by using *ab initio* Hartree-Fock calculations and a slab model. The model produced a rational explanation for the enhancement of tritium release by hydrogen. The hydrogen present in "pure" helium is at a level of a few parts per million. At this level, the surface coverage by chemisorbed hydrogen is too low to be effective in tritium removal. On the other hand, the extent to which tritium removal can be increased by adding hydrogen to the helium is limited due to a saturation effect when the surface sites favorable for hydrogen chemisorption become filled.

In another study, experimental and calculational methods were used to evaluate the probability and consequences of a water vapor reaction with Li_2ZrO_3 blanket material. The conclusion was that the thermodynamic stability of the Li_2ZrO_3 makes it an excellent candidate for use as a tritium breeder blanket.

Conceptual Processes for Tritium Recovery.

A detailed conceptual design of a tritium processing system for the $\text{Li}_2\text{O}/\text{Be}$ blanket was prepared for the design team of the International Thermonuclear Experimental Reactor. The functions of the system were to (1) recover and purify tritium from the two purge streams, (2) remove waste products from the streams and recover the tritium in the waste products, and (3) recirculate the purge streams to the blanket zones.

LITHIUM VAPORIZATION AND CORROSION

Tritium may be present in the form of LiOT within a ceramic breeder blanket and, under certain conditions of concentration and temperature gradients, may be transported to

cooler regions of the blanket. Preliminary experiments were performed to determine whether stainless steel components could be corroded by LiOT(g) and/or LiOH(g) from the blanket material. Lithium oxide (Li_2O) was placed under a stainless steel specimen, and helium containing a measured water vapor concentration was passed through the system at 750°C . Most of the LiOH(g) formed by reaction of the water vapor with the Li_2O reacted with the stainless steel sheet, and the remainder condensed in a cooler region downstream. The data showed that LiOH(g) does corrode structural stainless steel under fusion reactor conditions, and the reaction rate was inversely proportional to the distance between the stainless steel and the Li_2O breeder blanket material, and directly proportional to the LiOH(g) diffusivity in the carrier gas. The results of these experiments, together with other available information, were used to calculate possible corrosion of stainless steel by LiOT(g) from the Li_2O blanket planned for the International Thermonuclear Experimental Reactor.

Further studies on LiOH(g) vaporization showed that the potential problem was greatest for Li_2O breeder material, and less for other candidate materials (LiAlO_2 , Li_4SiO_4 , and Li_2ZrO_3). To assess the need for further experimental work in this area, existing literature data were expressed as a ratio of what would be predicted thermodynamically for equilibrium at the same temperatures and partial pressures of $\text{H}_2\text{O(g)}$. The conclusions from this comparison were that diffusional contributions to mass loss would be negligible and that a condition of thermodynamic equilibrium would prevail. Due to the consistency and replicability of the existing studies, further experimental work was deemed unnecessary.

Some additional work was done in 1995 on the compatibility of vanadium alloys for the

containment of ceramic breeder blanket materials (Li_2O , Li_2TiO_3 , and Li_2ZrO_3). Vanadium and its alloys were of interest because it is a low-activation material. A thermodynamic analysis was made in which equilibrium calculations were performed for the $\text{Li}_2\text{O/V}$ system. The results showed very little potential for the oxidation of vanadium. Similar results were found for the oxidation of vanadium by TiO_2 or ZrO_2 . On the basis of these results, no significant oxidation of the vanadium should occur by reaction with the lithium-bearing ceramic materials. There was some concern, however, that tritium could be released from the ceramic as condensable "tritiated water," which might react with the lithium oxide to form LiOH. Calculations using the SOLGAS computer code were applied to the various reactions that could be postulated for the system, and the general conclusion was that the partial pressure of moisture that could be formed could be very close to that required thermodynamically for vanadium oxidation.

PERSONNEL

The fusion work was under the direction of Carl Johnson in the 1990s. Other CMT personnel included Paul Blackburn, Rob Clemmer, Larry Curtiss, Pat Finn, Al Fischer, Larry Greenwood, John Kopasz, Vic Maroni, Shiu-Wing Tam, Erv Van Deventer, and Dai-Kai Sze. Much of this work was a cooperative effort with foreign scientists, who were coauthors of many of the publications. The secretary was Jan Carothers.

Applied Physical Chemistry

Work continued in the 1990s on several projects under this general category. Carl Johnson had the overall responsibility for these programs.

PHYSICAL PROPERTIES OF CORE-CONCRETE MIXTURES

Work continued up through 1992 on the thermophysical properties of molten mixtures of reactor core materials and concrete that could be formed in a severe accident involving the meltdown of a water-cooled nuclear reactor. The molten core-concrete interaction (MCCI) would be preceded by several other events: loss of coolant, heating and degradation of the core caused by fission-product decay, melting of the core debris (uranium oxide, fission products, Zircaloy cladding, control rods, and structural materials) through the stainless steel reactor vessel, and deposition of the core debris and molten steel on the concrete floor beneath the vessel. During the ensuing MCCI phase, the concrete basemat would react with the hot (~2700°C) core debris and steel to form a molten mixture of phases, which is vigorously agitated by the evolution of gaseous products (CO₂, CO, H₂O, and H₂) from decomposition and reduction of the concrete. Understanding and modeling the consequences of this kind of accident require a knowledge of the thermo-physical properties of the solids, liquids, and gases that are involved. Earlier studies of this subject were described in the previous chapter.

The results of this research were to be incorporated into thermal-hydraulic codes such as CORCON, which is an integral part of the Source-Term Code Package for the Nuclear Regulatory Commission. In brief, CMT contributed two important improvements to the computer models. The CORCON model had assumed that ideal liquid and solid solutions were formed in the reactions of the core material and concrete. The CMT experimental work showed that the system was much more complex than the ideal model, and that the temperature differences between the liquidus and solidus phases were much larger than had previously been

thought. The other contribution had to do with the viscosities of the mixtures. Experimental results showed that the viscosities of the mixtures were typically two orders of magnitude higher than the estimates that were being used in the CORCON code.

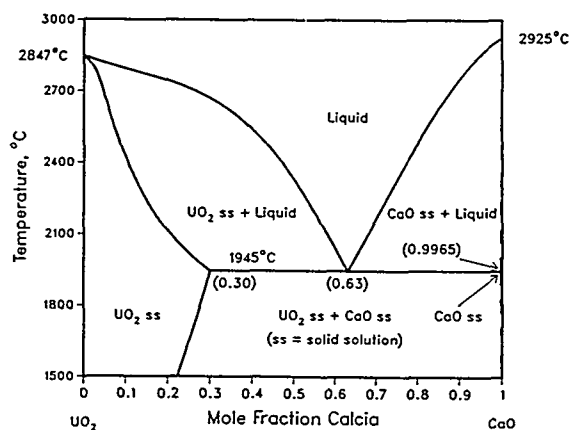
Differential Thermal Analysis Studies. Differential thermal analysis (DTA) measurements were used to determine the solidus-liquidus temperatures for three calcined concretes (limestone, limestone-sand, and siliceous) and mixtures of each of these with 73 wt% UO₂-ZrO₂. Measured differences between the solidus and liquidus temperatures for the three core-concrete mixtures were more than 1200°C, whereas the estimated differences using the CORCON code (for 27 wt% concrete) ranged between 500 and 700°C.

Experimental solidus and liquidus temperatures from the DTA measurements and calculated values from the literature are listed in Table 6-9 for mixtures of 27 wt% concrete with UO₂-ZrO₂ (mole ratio 1.6:1). In this case, the calculations were not based on ideal behavior. The measured and calculated results for the solidus values were in reasonable agreement. The disagreement between experimental and calculated liquidus values appeared to be roughly proportional to the calcia (CaO) content of the calcined concrete. The phase diagram of the UO₂-CaO system was redetermined (see Fig. 6-32), and incorporation of these new results into the calculations was expected to resolve the differences between the experimental and calculated results.

Viscosity Experiments. It is important to have reliable data on the viscosities of the products of core-concrete reactions because viscosity affects a variety of factors such as heat transfer, fission-product release, melt spreading, and cooling. Viscosity measurements were made on eight mixtures of

Table 6-9. Liquidus and Solidus Temperatures for Concrete-UO₂-ZrO₂ Mixtures

Concrete with UO ₂ -ZrO ₂	Solidus Temp., K		Liquidus Temp., K	
	DTA	Calculated	DTA	Calculated
Limestone	1520	1550	>2723	2320
Limestone-Sand	1360	1450	>2638	2490
Siliceous	1412	1434	2549	2395

Fig. 6-32. Phase Diagram for the UO₂-CaO System

UO₂-ZrO₂ and calcined concrete—one with siliceous concrete, four with limestone concrete, and three with limestone-sand concrete. The measurements were made with a Brookfield programmable viscometer equipped with a 70Mo-30W alloy rotating spindle. The measurements were made at temperatures extending from above the liquidus down into the liquidus-solidus range. In the liquidus region or with only a small volume fraction of solids, the fluid exhibited Newtonian behavior, *i.e.*, the viscosity was independent of the spindle rotation rate. At lower temperatures, where there was a higher volume fraction of solids, the behavior became non-Newtonian, *i.e.*, the viscosity decreased significantly with increasing

rotation rate (an effect known as “shear thinning”).

The results of these studies showed that the viscosities of core-concrete mixtures were significantly higher than values calculated by the thermal-hydraulic code, CORCON, which was being used to compute the consequences of hypothetical reactor accidents.

Personnel. Individuals involved in this research were Joanne Fink, Len Leibowitz, Mike Roche, Jack Settle, and Dave Steidl.

SUPPORT STUDIES FOR NEW PRODUCTION REACTOR (NPR)

In the U.S. nuclear weapons program, tritium is a vital material that can be produced in sufficient quantity and quality only by the irradiation of lithium in a nuclear reactor. Because tritium undergoes radioactive decay, a continuing supply is necessary not only to produce new weapons, but also to maintain existing ones. The DOE initiated the New Production Reactor (NPR) Program to plan, design, and build safe and environmentally acceptable new reactor capacity to ensure an adequate supply of tritium. The CMT Division supported this program by performing studies on a heavy-water-reactor NPR (HWR-NPR). This work involved the development of seals to meet stringent requirements for tritium containment in

process equipment and facilities, calculations of detritiation requirements in the event of accidental tritium releases into the containment structures, and calculational and experimental studies of fission-product release in a severe NPR accident.

Seal Design. Seal designs that are acceptable in normal commercial reactors fall far short of meeting the tritium-control requirements for an NPR. To achieve a desirably low level of tritium escape, the leak rates would have to be a factor of thirty or so lower than those for a commercial power reactor. The nuclear industry was already replacing asbestos valve packing and gaskets to meet EPA requirements, and graphite packing was coming into favor. A detailed study was made of state-of-the-art seal technology both in the U.S. and elsewhere. Detailed guidelines derived from this information were developed and published by Pat Finn (ANL-90/29). It appeared that additional capital costs of following these guidelines would be offset by lower operating costs and other benefits in long-term reactor operations.

Containment Habitability. The objective of this work was to develop an analytical approach to meeting the detritiation (decontamination from tritium activity) requirements in the event of an accidental tritium release within the containment structure. A critical factor is the time needed to reduce the activity in the containment structure to a level acceptable for human entry to perform maintenance or repair work without elaborate protective measures. The tritium activity in this situation was expected to be primarily in the chemical form of DOT. For the purpose of modeling, the containment structure was assumed to consist of concrete walls with an epoxy paint coating. The model could, however, accommodate other barrier materials. The

mathematical model, which was called the Dynamic Tritium Release and Analysis Model (DTRAM), simulated detritiation for either burst or chronic releases of tritiated species. The interactions included exchange, desorption, adsorption, dissolution, and bulk diffusion. The calculations showed that the time necessary to reduce the tritium levels to an acceptable value was dominated by the retention capability of the tritiated species in the structural materials. In spite of the fact that the tritiated species could, in principle, diffuse through the barrier materials to the external environment, the study indicated that virtually no such escape would occur.

Fission-Product Release from Fuels and Target in Severe Accidents. The purpose of this study was to develop a thermodynamic model that would predict the release of fission products and tritium from the Al-U fuel and Al-Li targets if the HWR-NPR had a severe accident. A review of the literature and preliminary transpiration experiments were conducted on aluminum alloys and an ingot prepared by Savannah River Laboratory that contained Al, U, Ba, C, Ce, Mo, Sr, and Zr in a helium stream to which 3% water vapor was added. At 873°C, the sample began to increase in weight, and when the sample was held at about 975°C for four hours, it oxidized at a decreasing rate with time.

Design Study on Modification of ANL-W Facilities for Tritium Recovery. A design concept was developed for modifications of a hot cell at ANL-W to handle irradiated fuel and target tubes in a tritium-controlled environment. No further work was done because of funding termination of NPR in the early 1990s.

Personnel. This work was performed by Rob Clemmer, Pat Finn, and Dai-Kai Sze.

THERMOPHYSICAL PROPERTY STUDIES

The fact that the driver (core) and blanket materials of the Integral Fast Reactor (IFR) were both U-Zr-Pu alloys made it highly desirable to have detailed, accurate information on the phase relations of this ternary system. Moreover, it was recognized that appreciable quantities of other actinides, including neptunium, americium, and curium, would grow into the fuel under irradiation, so data were also needed on the effects of small concentrations of these elements on the phase relations and other physical properties of the alloys. Possible interactions of constituents in the fuel cladding material (stainless steel) and the fuel components were of interest. The demise of the IFR program in the early 1990s lessened the urgency of these studies, and they were discontinued by 1996.

The U-Pu-Zr System. Calculation of the ternary phase diagram for the U-Zr-Pu system requires reliable information on the existence of all the phases present in the three binary subsystems, *i.e.*, U-Pu, U-Zr, and Zr-Pu, and their thermodynamic properties. In 1990, an extensive review of the literature was conducted to make a critical evaluation of the information that was available at the time. The calculations made use of the Facility for the Analysis of Chemical Thermodynamics (FACT) computer system, which was located in Montreal, Canada. Recalculation of the binary U-Pu phase diagram did not result in a major revision of the existing diagram, which is quite complex, but it did require some detailed changes to achieve thermodynamic consistency.

Subsequent investigations of the binary Pu-Zr system were done in much the same way as the U-Pu studies—a comprehensive evaluation of phase-equilibrium and thermodynamic data that were available in the literature on the Pu-Zr system. All the

literature data were well correlated by the thermodynamic analysis, using the FACT system, and reasonable, simple thermodynamic expressions were found for all the phases.

By 1995, a few new experimental results had become available on the U-Pu and Zr-Pu binaries. These were incorporated into a study that was aimed toward developing a set of model equations for the Gibbs energies of all phases as functions of composition and temperatures. All the thermodynamic properties and the phase diagrams could be calculated, and interpolations or extrapolations could be made in a thermodynamically correct manner. The Gibbs energy of the ternary solution phases can be represented by the Kohler equation, which is based upon an extension of regular solution theory:

$$\begin{aligned}
 G = & (X_{\text{Pu}}G_{\text{Pu}}^0 + X_{\text{U}}G_{\text{U}}^0 + X_{\text{Zr}}G_{\text{Zr}}^0) \\
 & + RT (X_{\text{Pu}} \ln X_{\text{Pu}} + X_{\text{U}} \ln X_{\text{U}} \\
 & + X_{\text{Zr}} \ln X_{\text{Zr}}) + (X_{\text{Pu}} + X_{\text{U}})^2 G_{\text{PuU}}^{\text{E}} \\
 & + (X_{\text{U}} + X_{\text{Zr}})^2 G_{\text{UZr}}^{\text{E}} \\
 & + (X_{\text{Zr}} + X_{\text{Pu}})^2 G_{\text{ZrPu}}^{\text{E}} + G_{\text{PuUZr}}^{\text{E}}
 \end{aligned}$$

where X is the atom fraction of species i , G_i^0 is the free energy of species i , G_{AB}^{E} is the excess free energy from the A-B binary system, and G_{ABC}^0 is the excess free energy from the ternary A-B-C system. All the available phase-equilibrium data in the Pu-U-Zr system were analyzed to determine optimized equations for the Gibbs free energies of all phases as functions of composition and temperature. The resulting calculated phase diagram was believed to be the best available estimate of the U-Pu-Zr system at the time. This was not only a highly useful tool for practical application of the data; it was also a very satisfying intellectual achievement.

The U-Fe-Zr System. As indicated previously, this system was of interest from the standpoint of possible fuel-cladding interactions in the IFR, with particular concern about reactions of iron in the stainless steel cladding (HT9, D9, or Type 316) with zirconium in the fuel alloy. The Fe-U phase diagram had been determined in considerable detail, but there were still some areas of uncertainty, particularly in the location of the liquidus curve. After some DTA measurements, the new data were incorporated into a recalculation of the U-Fe diagram, which then appeared to be a reasonable representation of the system.

A literature study of the binary Fe-Zr system showed two somewhat different phase diagrams. This system is fairly complex because it involves a number of solid-phase transitions and intermetallic compounds. The phase diagram was optimized by calculations based on Gibbs free energy data and the necessity for thermodynamic consistency. In general, all the available experimental data were incorporated successfully into the model, but some modifications were necessary to achieve thermodynamic consistency.

Studies were then extended to the ternary system, U-Fe-Zr. Again, the diagram for the ternary system was determined by calculating the excess Gibbs energies in the ternary liquid and the solid phases from values for the three subsidiary binary systems. Used for this calculation was the Kohler equation or the somewhat similar Toop equation. The following phases were considered in the calculations:

Liquid	U(γ)/Zr(β)	Fe ₂ Zr
Fe(γ)	Fe ₂ U	FeZr ₂
Fe(δ)	FeU ₆	FeZr ₃
Zn(β)	Fe ₃ Zr	

Two diagrams are possible, depending on whether Fe₂U and Fe₂Zr form a solid solution. The diagram based on the premise that such a

solid solution does not exist is shown in Fig. 6-33. If such a solution does exist, the isotherms and phase boundaries in the lower left portion of the diagram are shifted slightly. It may be the case that reality lies somewhere between these two possibilities, that is, a partial solid solubility may be involved.

Minor Actinide Systems. During the operation of an IFR, the transuranic elements (Np, Pu, Am, and Cm) are formed in the fuel due to neutron capture. The lighter elements (Np, Pu), because their 5f electrons interact strongly with the 6d and 7s electrons, tend to behave chemically like uranium. In the heavier elements (Am and Cm), however, the 5f electrons are more localized, and they tend to act like the rare earths. This effect also influences the metallurgical as well as the chemical properties of Am and Cm, and this is reflected in the crystal habits of the metals. Although some lanthanide and actinide binary phase diagrams pertinent to the IFR were available, the absence of experimental data in this area forestalled application of the usual thermodynamic modeling and phase-diagram optimization methods, and the situation was

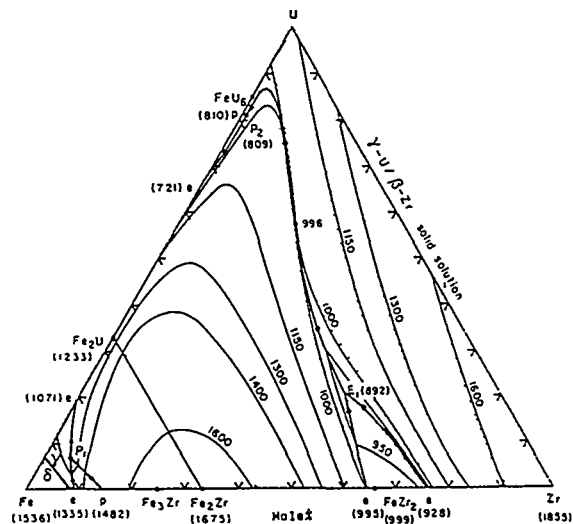


Fig. 6-33. Liquidus Surface of Calculated Fe-U-Zr Phase Diagram

made worse by the extraordinary complexity of the actinides. Application of several alternative modeling approaches met with mixed success, but the results did not engender a high confidence level.

Materials Data Base. A data base on the properties of IFR materials that had been generated in collaboration with the Fuels and Engineering (FE) Division in 1988 was updated in 1993. Data on vapor pressure, heat capacity, density, compressibility, surface tension, thermal conductivity, viscosity, and related properties of sodium were added to the data base. Updates were also made on plutonium phase transitions and thermal conductivity and thermal diffusivity of U, Pu, Zr, and alloys of these elements. A significant conclusion from this effort was that much more information was needed on thermal conductivities, diffusivities, and certain other properties of plutonium and its alloys.

Personnel. Involved in this work were Bob Blomquist, Joanne Fink, Len Leibowitz, and Ewald Veleckis.

DEVELOPMENT OF SYNCHROTRON ANALYTICAL CAPABILITIES

In 1984, CMT began collaborating with Louisiana State University (LSU) to build a synchrotron X-ray beamline at the Center for Advanced Microstructures and Devices (CAMD). This program grew out of earlier work in which a team of Argonne researchers developed methods to investigate small-scale structures, using the National Synchrotron Light Source (NSLS) at Brookhaven National Laboratory. By using a combination of X-ray fluorescence and diffraction, information on sample composition and structure can be determined simultaneously. Hardware and software for the system were developed and tested. This work was expected to lead to a unique facility for microscopic X-ray

examinations in a wide variety of applications. Various people were involved in these studies, including Len Leibowitz, Carlos Melendres, and Zoltan Nagy.

Basic Chemistry Research

In the early 1990s, Vic Maroni and Milt Blander were in charge of the basic research programs. Vic was in charge of all the basic studies, which fell under the general purview of the CMT department headed by Mike Myles. In 1998, Zoltan Nagy and Larry Curtiss were transferred to other ANL divisions, at considerable loss to the CMT basic research programs.

PHYSICAL ORGANIC CHEMISTRY

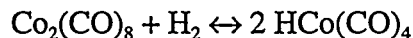
The fluid catalysis work continued under the leadership of Jerry Rathke in the 1990s, and Hal Feder, although retired to Florida, also kept in touch with the program, largely through e-mail, essentially up to the time of his death in 1997. The fluid catalysis work included four types of investigations: (1) catalytic reaction chemistry of small molecules (CO , CO_2 , CH_4 , and H_2) that serve as precursors in the industrial production of useful products, (2) hydrocarbon activation to achieve the controlled catalytic reactions of methane and other hydrocarbons by activation of their C-H bonds, (3) organometallic C-H activation chemistry in the production of carbide-containing fibers, films, or larger objects, and (4) the mechanism(s) of ion transport in lithium-polymer batteries.

Catalytic Chemistry in Supercritical Media. Over 90% of industrial chemical processes entail the use of catalysts, and nearly half of these are homogeneous catalytic processes in which the catalyst is dissolved in a fluid (typically an organic solvent). Although these systems offer high reactivity, selectivity, and relative ease of modification for special

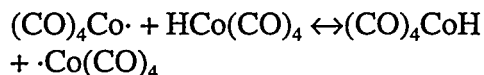
purposes, catalyst recovery and product separation often present problems. Supercritical fluids such as CO₂ or H₂O appear to be environmentally benign alternative solvents that would eliminate the use, storage, handling, and disposal problems associated with organic solvents. Supercritical fluids, because of their gas-like transport properties, complete miscibilities with gases, and sharp changes in dissolving power with fluid density, have the potential both for accelerating diffusion-controlled reactions of gases with liquid and solid substrates and separating catalysts or catalytic products by energy-efficient pressure alterations.

The "oxo" process for the hydroformylation of olefins is the largest scale production process using homogeneous catalysis. In this process, CO and H₂ react with an olefin in the presence of a soluble catalyst to produce aldehydes and alcohols for detergents, plastics, and agricultural products. *In situ* nuclear magnetic resonance (NMR) studies were conducted to determine the effects that the use of supercritical media would have on the various equilibrium and kinetic factors in the process. The NMR probe is capable of operating at temperatures up to 300°C and pressures up to 34 MPa (5,000 psi). The solubility of Co₂(CO)₈ in supercritical CO₂ was measured, and the entropy and enthalpy of dissolution were derived: 20 ± 1.7 kJ/mol and 30 ± 4 kJ/mol·K, respectively. It is interesting that these experimental measurements, unlike those in most catalysis research, were made much easier by the fact that only a single phase was present. Additional detailed information was obtained on intermediate species, rate constants, *etc.*, and some experimental information was obtained on the formation of butyraldehydes by hydroformylation of propylene. A significant result of this study was that the ratio of n-butyraldehyde to i-butyraldehyde in the product was different with supercritical CO₂ than it was for conventional solvents.

During the investigations of propylene hydroalkylation in supercritical CO₂ with the Co₂(CO)₈ catalyst, the NMR results suggested that a tetracarbonyl radical, HCo(CO)₄·, may have had a role in the reactions. Spectra that were recorded at varied temperatures during the hydrogenation of Co₂(CO)₈ provided enthalpy and entropy data for the reaction



Broadening and coalescence of the resonance peaks for HCo(CO)₄ and Co₂(CO)₈ were attributed to a second step in the process:



Even more convincing evidence for the existence of this radical was obtained by isotopic exchange of ¹³C between CO and Co₂(CO)₈, which probably occurs through the radical. Additional studies were made with Mn₂(CO)₁₀, which is similar to Co₂(CO)₈, although less effective in its catalytic behavior. It had been studied as a model for certain steps in the commercial cobalt carbonyl process. The results of these studies were consistent with those from the cobalt compound, and an interesting additional finding was that Co₂(CO)₈ and Mn₂(CO)₁₀ form the mixed dimer (CO)₅Mn-Co(CO)₄.

Results from NMR measurements of magnetic susceptibilities of solutions containing Co₂(CO)₈ at different temperatures were used to obtain thermochemical data on pertinent bond energies in the system. The enthalpy and entropy changes for the Co-Co bond were 80 ± 8 kJ/mol and 121 ± 17 J/mol·K, respectively. The H-Co bond energy was 248 ± 4 kJ/mol, which seemed more reasonable than an electrochemically determined value of 260 kJ/mol.

The total world capacity of the oxo process for the hydroformylation of olefin is about

5 million tons per year. The phosphine-modified cobalt hydroformylation process was invented by, and is used exclusively by, the Shell Chemical Company. Preliminary high-pressure NMR experiments showed that many of the organometallic species could be observed and quantified by NMR with phosphorus-31. One of the conclusions from these measurements was that the Co-Co bond in the phosphine-substituted dimer is stronger than that in $\text{Co}_2(\text{CO})_8$. These *in situ* NMR measurements were made at temperatures of 75 to 225°C and initial H_2 and CO partial pressures of 6.9 MPa. Further studies were made on the effect of CO pressure on the compositions of the cobalt species present in the catalytic solutions of the tributylphosphine-modified catalyst, $[\text{Bu}_3\text{PCo}(\text{CO})_3]_3$. High CO pressures result in the formation of a salt, $[(\text{Bu}_3\text{P})_2\text{Co}(\text{CO})_3]^+ + [\text{Co}(\text{CO})_4]^-$. Because the salt would be expected to be inert, use of high CO pressures to encourage catalyst formation would be counterproductive.

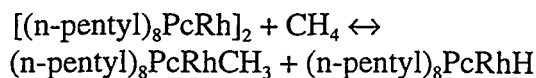
In recent studies, the first thermodynamic measurements were completed on the key equilibria associated with phosphine-modified hydroformylation catalysis of the type used commercially. Equilibria were measured not only on the catalyst hydrogenation step, but also carbon monoxide-induced salt formation, which has so far prevented the reaction from being conducted in a supercritical fluid. The results suggest that phosphines having lower basicity might make such reactions in supercritical fluids possible for the first time. This discovery could have important commercial applications.

Hydrocarbon Activation Chemistry. The objective of this continuing research was to investigate the activation of hydrocarbons by using soluble metallophthalocyanines (MPc) as the catalysts. Although the MPc catalysts were well known for their catalytic activities on the autoxidation of hydrocarbons, the

mechanisms for these reactions were not well understood. A Rh-Rh bonded dimer, $[(\text{R}_8\text{Pc})\text{Rh}]_2$, where R_8Pc^{2-} is the dianion of 1,4,8,11,15,18,22,25-octapentylphthalocyanine, was synthesized and shown to react with H_2 and CH_4 to form the products $(\text{R}_8\text{Pc})\text{RhH}$ and $(\text{R}_8\text{Pc})\text{RhCH}_3$, respectively. The lower the Rh-Rh bond energy, the more active the dimer $[(\text{R}_8\text{Pc})\text{Rh}]_2$ is for activating CH_4 and other hydrocarbons. Homolysis of the rhodium dimer to form $(\text{R}_8\text{Pc})\text{Rh}\cdot$ radicals was proposed to explain the experimental observations.

At 180°C, the rhodium dimer catalyzed the H-D exchange reaction between D_2O and both the aromatic and the alkyl hydrogens of the R_8Pc^{2-} ligand to form the $(\text{R}_8\text{Pc})\text{RhD}$ complex. The catalytic chain mechanism for the H-D exchange between D_2O and the alkyl hydrogens was worked out. Further studies of the $(\text{R}_8\text{Pc})\text{RhH}$ complex showed the existence of two isomers, monomeric $(\text{R}_8\text{Pc})\text{RhH}$ and dimeric $(\text{R}_8\text{PcH})\text{Rh}-\text{Rh}(\text{R}_8\text{PcH})$. Also prepared and isolated were $(\text{R}_8\text{Pc})\text{LRh}\cdot$ radicals where L represents trimethyl or tributyl phosphine.

An effort was then focused on the use of catalytic complexes containing rhodium centers bound to solubilized phthalocyanine (Pc) ligands. The rhodium center has an ability to form reasonably strong, but still reactive, metal-carbon and metal-hydrogen bonds. Methane was activated by using a metal-metal bonded rhodium Pc dimer that interacted with methane by the equilibrium reaction



Several approaches to the synthesis of phthalocyanines, as well as the use of molecular mechanics, were combined with semiempirical molecular orbital calculations to evaluate various types of substituents for use as spacers. (Alkyl substitutes on the

phthalocyanine nucleus serve both to solubilize the complexes and to provide spacers that weaken, and thereby activate, the Rh-Rh bond in the dimer by steric repulsions between the linked macrocycles.) Figure 6-34 compares models of phthalocyanine frameworks determined by X-ray measurement (upper figure) and by molecular modeling calculations (lower figure). The two models are in close agreement. The X-ray model, however, shows an unusual feature in that the presence of substituents results in distortions such that one of the benzpyrrole groups is twisted out of the molecular plane by 15°. Apparently, the stress introduced by long-chain alkyl substituents is relieved by out-of-plane bending of one pyrrole group.

Further studies showed that soluble rhodium complexes in which the n-pentyl groups were replaced by trifluoromethyl groups can be synthesized, for example, $(CF_3)_8PcRhOCH_3$. With these fluorocarbon constituents, the metallophthalocyanines can be tailored to very high electrophilicities, which, together with their high thermal and

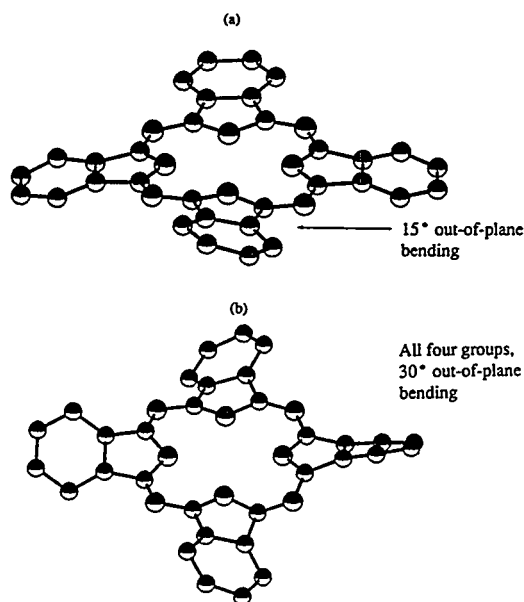
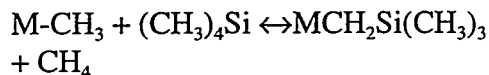


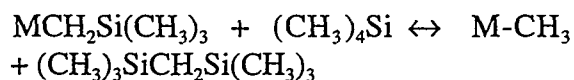
Fig. 6-34. Models of Phthalocyanine Frameworks

oxidative stabilities, open up the potential for a wide variety of homogeneous catalytic oxidations, oxidative couplings, substitution reactions, and other useful hydrocarbon conversion processes. A dimeric oxo-bridged iron complex of a highly fluorinated phthalocyanine ligand was synthesized, and it proved to be an effective catalyst for the epoxidation of olefins and the hydroxylation of alkanes.

Ceramic Precursor Research. The objective of this research was to explore novel catalytic methods for the synthesis of organometallic polymers from small precursor molecules. The idea was to apply C-H bond activation chemistry to organometallic substrates and to explore the chemistry of organometallic polymers and their ceramic-forming mechanisms. This type of work could lead to improved processes for the preparation of coatings, whiskers, fibers, or even larger three-dimensional ceramic objects. Carbides of Si, B, W, Ti, and other metals have superior hardness, high tensile strength, and other desirable properties for many applications, but they are difficult to fabricate in useful shapes. An attractive approach to this problem would be to synthesize pre-ceramic polymers that could be formed readily into the desired shapes, and then fire the material to form the ceramic. This general approach is being used commercially for the production of high-strength SiC fibers.

A catalytic strategy was devised for the polymerization of small organometallic molecules such as tetramethylsilane. In principle, this approach should lead to polymers having an alternate arrangement of metal and carbon atoms. This strategy is based on two reactions:





where M is an electrophilic metal center in an early transition metal or lanthanide or actinide complex. Both of these reactions were well-known, and the product has the desired alternating arrangement of Si and C atoms. The catalyst, M-CH₃, is consumed in the first reaction and regenerated in the second one. Steps analogous to those in these reactions can bring about further reactions of dimer and higher oligomers. Such reactions lead to polymerization and cross-linking or branching that can be controlled by the steric requirements of the catalyst. Oligomerization of both tetramethylsilane and trimethylaluminum was achieved, and the products had the desired alternating arrangement of metal and carbon atoms.

A magnetic resonance imaging device that appears to offer the means for excellent characterization of advanced materials and materials chemistry processes in this technology was based on the toroid detectors used with high-pressure NMR probes. This toroid cavity imager proved to be extremely useful in obtaining (1) NMR spectra on different regions of a flame, (2) structure or composition on the different layers of a thin film or coating, (3) the penetration depth or diffusion rate of a fluid into a porous substrate at high pressures, and (4) concentration gradients of various species near an electrode of an electrochemical cell. In 1994, some new 180° pulse sequences were developed, which almost completely compensate for the radio-frequency field gradient within the torus. This development greatly extended the scope of applications for NMR imaging.

Determination of Ion Transport by NMR Imaging. Although nuclear magnetic resonance is a powerful tool for determining chemical structure and reaction dynamics, the distance resolution of standard magnetic

resonance imaging is gained only at the expense of sacrificing the chemical structure and reaction dynamics information. For this reason, it was not well suited to examination of the processes occurring in electrochemical systems on a micro scale very close to the electrode surfaces, which is the region of most interest. A new analytical technique was developed, in which the distance resolution of the NMR imaging method was close to the micron scale, which is sufficient to resolve most of the electrochemical details of interest while retaining all the NMR chemical shift, coupling constant, and relaxation time information. This new technique was based on the toroid cavity detector that was used earlier in the *in situ* NMR work on fluid catalysis at high temperature and pressure.

A schematic diagram of the electrochemical NMR imaging device is shown in Fig. 6-35. The central conductor served both as the electrochemical working electrode and as the central wire in the NMR detector circuit. The first application of this device was to investigate the mechanism(s) of lithium ion transport in lithium-polymer electrolyte batteries, which were discussed earlier. Lithium-ion mobility depends upon its diffusion coefficient, the overall ionic conductivity, and the lithium-ion transference

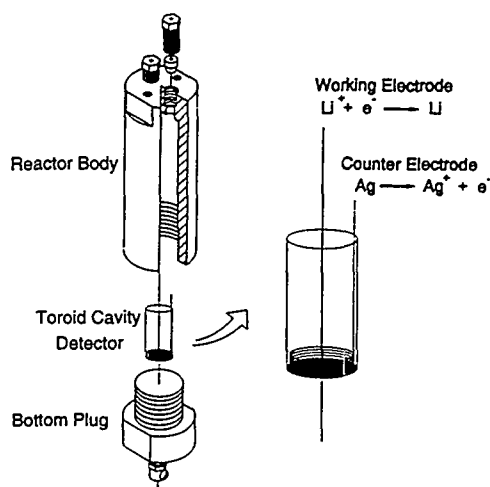


Fig. 6-35. Electrochemical-NMR Imaging Device

number (the fraction of the current carried by lithium ions). The transference number was the primary focus of this work because it was the item of greatest uncertainty.

The electrochemical NMR imaging technique was used to measure lithium-ion concentration profiles in the electrolyte depletion area at the electrode surface as a charge was passed through the cell containing a sample of $\text{CF}_3\text{SO}_3\text{Li}$ in polyethylene oxide. From the amount of electrical charge passed through the cell and measurements of the electrolyte depletion zone (which was about 0.5 mm), the lithium-ion transference numbers could be calculated. In addition to transference numbers, lithium-ion diffusion coefficients could be measured by imaging the salt depletion zone after various time intervals. The results of ongoing studies of the polymer electrolyte batteries showed that the lithium-ion transference numbers and lithium-ion diffusion rates were both very low. This condition severely limited the thickness of the polymer film that was utilized. To develop a battery with adequate performance, it appeared that modifications would be necessary in the electrolyte systems.

Personnel. Jerry Rathke was in charge of this work, which also included Mike Chen, Bob Klingler, and others.

HIGH T_c SUPERCONDUCTORS

The excitement that had been generated by the discovery of solid oxide systems that are superconductive at considerably higher temperatures than the earlier metallic systems continued into the 1990s. Unlike the earlier materials, which were superconductive only up to a temperature of about 10 K, these oxides showed superconductivity at temperatures approaching 100 K. This means that they could find practical application in devices cooled by liquid nitrogen, which is widely used in industry for cryogenic

purposes. The CMT work in this area was in cooperation with the American Semiconductor Corp., Radiation Monitoring Devices, Inc., and the ANL Materials and Components Technology Division.

Structural Transitions and Thermodynamic Behavior. This research was focused on the structural transformations and the nonstoichiometric and thermodynamic behavior of high- T_c superconducting oxide systems such as $\text{YBa}_2\text{Cu}_3\text{O}_x$. These properties were determined as a function of oxygen partial pressure, oxygen stoichiometry, and temperature by coulometric titration in which the oxygen content was varied by well-defined small amounts. Earlier electromotive force (emf) measurements on $\text{YBa}_2\text{Cu}_3\text{O}_x$ had shown a miscibility gap centered at $x = 6.65$ with a consolute temperature of 473 K. The objective of the present study was to investigate the effects of ionic size of Ln^{3+} (where $\text{Ln} = \text{Y}, \text{Gd}, \text{or Nd}$) on the structural transitions and thermodynamic and nonstoichiometric behavior in the $\text{LnBa}_2\text{Cu}_3\text{O}_x$ system.

Equilibrium oxygen pressures were calculated from the emf data for isotherms in the temperature range of 673-873 K as a function of x in $\text{NdBa}_2\text{Cu}_3\text{O}_x$. The partial pressures turned out to be higher than those reported earlier for the $\text{YBa}_2\text{Cu}_3\text{O}_x$ system. These results were consistent with the change in the observed composition dependence of T_c on ionic radii for Y and Nd in $\text{YBa}_2\text{Cu}_3\text{O}_x$ and $\text{NdBa}_2\text{Cu}_3\text{O}_x$. Two plateaus of T_c suggest the presence of phase separation in a miscibility gap, which would operate for the yttrium phase, but not for the neodymium phase. If a miscibility gap were present in the neodymium system, it would occur at a much lower temperature and higher value of x than in the yttrium system.

The thermodynamic and structural studies were then turned toward the high T_c system, $(\text{Bi}_{2-x}\text{Pb}_x)\text{Sr}_2\text{Ca}_2\text{Cu}_3\text{O}_y$ (Bi-2223), which was

being used for the fabrication of silver-sheathed superconducting wire. Electromotive force measurements were used to measure oxygen fugacities as a function of oxygen stoichiometry, and a coulometric titration was made to investigate the thermodynamic behavior of the material as a function of oxygen partial pressure, oxygen stoichiometry, and temperature. The limiting stability condition at low oxygen partial pressure was the $\text{CuO-Cu}_2\text{O}$ phase boundary.

Further investigations of Bi-2223 were performed with a sample of the material prepared at Ames Laboratory, and another one prepared at ANL. Oxygen partial pressures were determined as a function of oxygen stoichiometry, the value of x in $(\text{Bi,Pb})_2\text{Sr}_2\text{Ca}_2\text{Cu}_3\text{O}_x$. The measurements gave reproducible results that defined the stability region for single-phase Bi-2223 as existing between oxygen partial pressures of about 0.02 and 0.20 atm. Differential thermal analysis and X-ray diffraction indicated that decomposition of the material at oxygen pressures below about 0.001 atm produces $(\text{Bi,Pb})\text{Sr}_2\text{CuO}_x$, $(\text{Ca,Sr})_2\text{CuO}_3$, and Cu_2O . The conclusion from these results was that Pb-doped Bi-2223 should remain as a single-phase material during processing or annealing at 750-800°C and oxygen partial pressures of about 0.02 to 0.20 atm.

A comparison was made between the oxygen partial pressures of lead-doped and lead-free Bi-2212. The results showed a narrower range of stability for lead-free Bi-2212 than that for lead-doped Bi-2212 and Bi-2223.

Development of High- T_c $(\text{Bi,Pb})_2\text{Sr}_2\text{Ca}_2\text{Cu}_3\text{O}_x$ Wires. Collaborative research with the American Superconductor Corp. was performed on the growth and stability of high- T_c phases in the lead-doped Bi-Sr-Ca-Cu-O system. The goal of this work was to establish the synthesis and processing procedures that would have the greatest effect on the critical

current properties of metal-sheathed high- T_c conductors. The growth and stability of the Bi-2223 phase fabricated into silver-sheathed wires were investigated by a combination of X-ray diffraction, scanning electron microscopy, energy dispersive X-ray analysis, and transmission electron microscopy. During the fabrication, a precursor powder, $(\text{Bi,Pb})\text{Sr}_2\text{CaCu}_2\text{O}_x$ (Bi-2212), was converted to the Bi-2223. Modeling of the equilibration data indicated that the Bi-2212→Bi-2223 conversion was controlled by two sequential kinetic regimes—a liquid-phase diffusion process and a solid-state process. Data for fractional conversion to the Bi-2223 phase vs. time correlated best with a two-dimensional, diffusion-controlled mechanism that had an unusually large activation energy (>1 MJ/mol). The temperature and the oxygen pressure had a somewhat complex competing effect, and the XRD data showed grain alignment of the Bi-2223 crystals in the silver-clad wires, and the alignment was greatly enhanced during rolling or pressing of the wire. Tests of silver-sheathed Bi-2223 wires prepared by the ANL Materials and Components Technology Division showed that the conditions used for calcining the precursor Bi-2212 plus secondary phases had an effect on the alkaline earth cuprate secondary phases, which, in turn, had a pronounced effect on the rate and course of Bi-2223 formation.

Preparation of High- T_c Films by Alloy Oxidation. This effort was aimed toward the development of methods to prepare high- T_c superconducting films by oxidizing liquid alloy precursors. Earlier studies had shown that liquids having the composition MBa_2Cu_3 , where $M = \text{Eu}$ or Yb , and a melting point <1173 K could be oxidized to produce textured films of $\text{MBa}_2\text{Cu}_3\text{O}_7$ (123) if the liquid metal was supported on a suitable single-crystal substrate such as SrTiO_3 (100). The resulting high- T_c films showed a

preferential orientation of the 123 phase a-b planes parallel to the substrate surface and achieved critical current densities in the range of 10^4 to 10^5 A/cm². A goal of the study was to find less expensive substrate materials and 123 materials more abundant than europium or ytterbium.

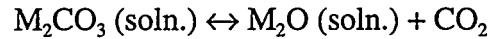
A collaborative research effort was established with American Superconductor Corp., and a specially designed high-temperature, high-vacuum apparatus was used for this work. When a highly oriented film of YbBa₂Cu₃ was applied to the single-crystal substrate by dipping, the high-T_c film was about 10 μm thick and had a strong c-axis orientation perpendicular to the substrate surface when the substrate was SrTiO₃ (100) or MgO (100). Microscopic and microprobe examinations revealed regions of near-epitaxial ordering of the high-T_c material within about 5 μm of the interface. These research studies were completed in 1991, when the processing parameters had been refined to the stage where high-quality, epitaxial YbBa₂Cu₃O_x films, 10 to 20 μm in thickness, could be prepared. The critical temperature and current density were ≥80 K and about 1000 A/cm², respectively.

Personnel. This was an interdivisional project. The CMT portion of the work was led by Vic Maroni, and included the efforts of Milt Blander, Ira Bloom, Alan Brown, Larry Curtiss, Al Fischer, Dieter Gruen (CHM), Mark Hash, Stan Johnson, Jian Shu Luo, Shiu-Wing Tam, and Ben Tani, as well as some part-time people.

ORDERING AND ASSOCIATION IN LIQUIDS

Solubilities of NiO in Molten Carbonates. In molten carbonate fuel cells, dissolution of the NiO cathode and its transport to the cathode in the 62 mol% Li₂CO₃-38 mol% K₂CO₃ molten salt electrolyte were a frequent cause

of cell failure. Measurements of the solubility of NiO in alkali carbonates were analyzed to develop a better understanding of the chemistry involved and thereby aid in improving cell performance. The following equilibrium exists for an alkali carbonate:



where the activity of the alkali oxide, M₂O (where M is Li, Na, K, or Rb), increases with a decrease in CO₂ pressure. At a given pressure, the oxide concentration is highest in Li₂CO₃ and lowest in Rb₂CO₃. The NiO solubility data were consistent with the presence of the three species Ni²⁺, NiO, and NiO₂²⁻. The major species in fuel cell electrolytes at 700°C and CO₂ pressures ≥1 atm is Ni²⁺, *i.e.*, NiCO₃. With solid NiO present at the electrode and a constant CO₂ pressure, the NiCO₃ concentrations and NiO solubilities are inversely proportional to the activity coefficient of NiCO₃, which is highest in Li₂CO₃ and lowest in Rb₂CO₃.

Conformal Ionic Solution Theory for Aqueous Electrolytes. The Conformal Ionic Solution (CIS) Theory, a statistical mechanical perturbation theory that had been applied primarily to molten salt systems, was mentioned in previous chapters. When applied to aqueous systems, the simplest reciprocal salt system consists of two cations (A⁺, B⁺), two anions (X⁻, Y⁻), and the dielectric solvent, H₂O. Equations were derived for the Gibbs energies and enthalpies of mixing for the quaternary solutions. These equations can be used to calculate the thermodynamic properties of quaternary solutions from those of the lower-order binary and ternary subsystems.

Structures of Molten Salts. Experimental studies were continued on the melting mechanisms of trivalent metal halides. The two compounds, YCl₃ and AlCl₃, are

interesting in that they have the same crystalline structure, but differ markedly in many of their physical properties, including melting points (YCl_3 melts at 721°C , while AlCl_3 sublimates at 193°C). Large differences also exist in the entropies of melting, the electrical conductivities, and the volume changes on melting. The Intense Pulsed Neutron Source (IPNS) at ANL was used to study the structure of YCl_3 . The compound AlCl_3 was well known to form a liquid structure totally different from the crystal structure. The liquid consists of molecular Al_2Cl_6 units with two tetrahedra sharing a common Cl-Cl edge and an Al-Cl coordination number of four. The YCl_3 , upon melting, retains its octahedral character in a loose arrangement with a coordination number of 5.8.

This work was a cooperative effort of CMT researchers, in particular, Milt Blander, plus David Price of the ANL Materials Science Division (MSD), and M. Tosi of the International Center of Theoretical Physics, Trieste, Italy.

Personnel. Milt Blander and Marie-Louise Saboungi have provided the impetus for these investigations. Other CMT members involved in the work were Ira Bloom, Larry Curtiss, and Jerry Johnson. As in most of the other basic programs, much of the effort was by part-time people and collaborators at other institutions.

QUANTUM CHEMICAL STUDIES

The use of quantum mechanics, in the form of *ab initio* molecular orbital calculations, to determine structural and thermochemical characteristics of compounds and other entities began in CMT in the calorimetry and thermochemical properties programs and soon found application in many of the Division's other research and development programs. This discussion concerns studies that were of

more general scientific interest. In 1990, the Gaussian-2 (G2) theoretical procedure was developed for calculating molecular energies of compounds containing first row (Li→F) and second-row (Na→Cl) atoms. The G2 procedure is a refinement of the G1 procedure, which is based on Hartree-Fock theory and includes high levels of correlation energy, as well as quadratic configuration interactions and large basis sets. The G2 procedure involves corrections to various basis set extensions and gives improved calculated values in comparison with well-established experimental values for atomization energies, ionization potentials, electron affinities, and proton affinities for a large number of species. Larry Curtiss performed many of these calculations, which contributed to a much better understanding of structural aspects of the chemistry involved in a wide variety of CMT programs. Larry's work in this area received wide recognition, and he has been a collaborator and coauthor of many publications with Dr. John A. Pople of Northwestern University, who was awarded a Nobel prize in chemistry for this type of work in 1998.

The new procedure was tested on atomization energies of 125 molecules with an average deviation from experimental data of 5.06 kJ/mol, and it was used successfully to test uncertain data on 79 molecules. Methods were also developed for third-row non-transition metals (Ga→Kr). The increase in binding energy of silicon clusters (Si_n) as more silicon atoms were added to the cluster was calculated, and the results agreed with experimental data for $n = 2-3$. In work related to studies of methanol in the ANL Chemistry Division, calculations by CMT researchers showed that the literature value for the ionization potential of the methoxy radical was in error by about 3.5 eV, and that the established experimental C-H bond dissociation energy of methanol was in error. The G2 theory was also used to investigate silicon